AD-A177 683 SUITABILITY AND APPLICATIONS OF LIQUID CRYSTAL TELEVISIONS IN OPTICAL PRE-PROCESSORS(U) AIR FORCE INST OF TECH WRIGHT-PATTERSON AFB OH SCHOOL OF ENGI. 1/1

UNCLASSIFIED K D HUGHES DEC 86 AFIT/GE/ENG/86D-6 F/G 17/2 NL

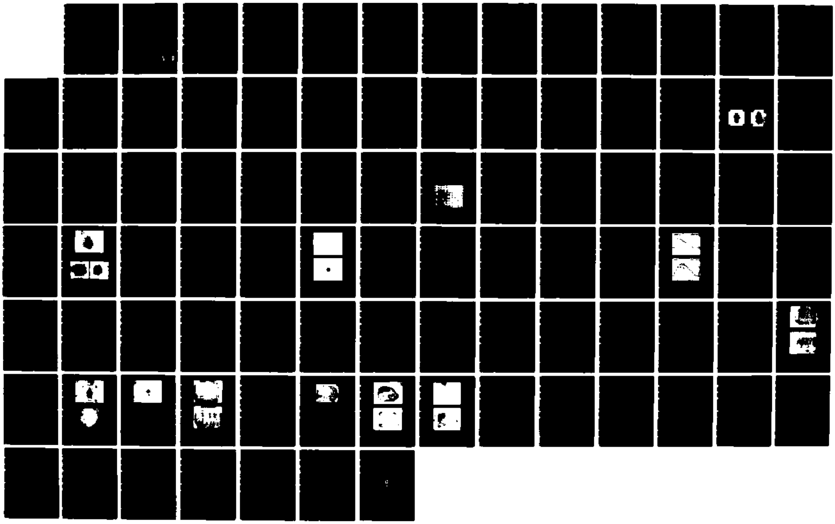

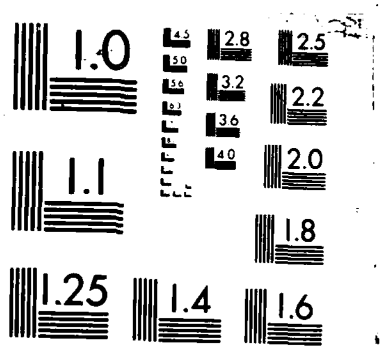

MICROCOPY RESOLUTION TEST CHART
NATIONAL BUREAU OF STANDARDS 1963 A

Suitability and Applications of Liquid Crystal Televisions In Optical Pre-processors

THESIS

Kenneth D. Hughes
Captain, USAF

AFIT/GE/ENG/86D

DEPARTMENT OF THE AIR FORCE
AIR UNIVERSITY
AIR FORCE INSTITUTE OF TECHNOLOGY

Wright-Patterson Air Force Base, Ohio

AFIT/GE/ENG/86D-6

Suitability and Applications of Liquid Crystal Televisions In Optical Pre-processors

THESIS

Kenneth D. Hughes
Captain, USAF

AFIT/GE/ENG/86D

AFIT/GE/ENG/86D-6

Suitability and Applications of Liquid Crystal Televisions In Optical Pre-processors

THESIS

Presented to the Faculty of the School of Engineering

of the Air Force Institute of Technology

Air University

In Partial Fulfillment of the

Requirements for the Degree of

Master of Science in Electrical Engineering

Kenneth D. Hughes, B.S.E.E.

Captain, USAF

December 1986

Approved for public release; distribution unlimited

Preface

The idea of researching the use of the liquid crystal televisions in an optical pre-processor for an electrical pattern recognition system was first introduced to me by my advisor Dr Steve Rogers and Dr Jim Mills. The combination of this with the application of edge enhancement made the research very interesting and informative as well as practical.

I have had a lot of help and encouragement with my work on this thesis. I would like to thank my advisor Dr Rogers and also the members of my committee, Dr Mills and Dr Kabrisky for their very patient and understanding help. I would also like to thank Dick Lane, Dale Stevens, and Jim Heitman of the Electronic Technology Division of the Air Force Avionics laboratory for their support and advice. They were very supportive and really fantastic when it came to providing me with the necessary equipment. Finally, I would like to thank my wife, Sheryl for her patience and the Lord God for blessing my family during this time.

Table of Contents

Table of Contents

List of Figures

List of Figures

Abstract

The suitability of a low-cost liquid crystal television to function as a spatial light modulator for lasers is investigated along with an application of using such a modulator in an optical pre-processor for an electronic pattern recognition system. The particular pre-processor application investigated is that of optically enhancing the edges of an image. It was determined that the liquid crystal television could perform reasonably well as a spatial light modulator for applications where very high image quality was not required. Three different methods were found to produce recognizable edges of a given image: spatial filtering in the Fourier plane, image cancellation, and phase cancellation. The phase cancellation method was discovered during the course of the research. These methods were able to perform the edge enhancement task whether the image was binary as in a computer generated image, or was continuous as from a television camera.

I. Introduction

The purpose of this thesis is to investigate the suitability of low-cost liquid crystal televisions, currently available, to function as a spatial light modulator for lasers. This function would make them very useful in studying optical pre-processors which can be used in conjunction with digital computers to make certain computing tasks less time consuming. In addition, this thesis will investigate the particular application of using the liquid crystal television in an optical pre-processor for a digital pattern recognition system.

Overview

A current topic of great interest to the Air Force, as well as the scientific community, is that of automatic pattern recognition. This topic is of particular interest to the Air Force due to the potential applications in automatic target recognition, which can be employed in autonomous weapons (13:3579). Automatic pattern recognition also has important applications in robot vision systems (9:445). Many implementations of the recognition of patterns in images, though, are presently done almost exclusively by computer. Even with the high speeds capable in modern computers, the shear enormity of the pattern

recognition task can make it a time consuming one. One proposal for speeding up this task is to allow some of the computing to be done optically 'at the speed of light' as will be discussed in this thesis (7:69).

With automatic target recognition, a so-called 'smart' weapon such as a missile could be launched into a target-rich area and programmed to search for an enemy target. This missile would then start searching for the desired type of target, such as a tank, with various types of detectors. One popular technique is to use optical detectors which digitize a received image and feed it into an on-board computer for recognition (10:227). The problem with this technique of pattern recognition is that the computations involved in recognizing an object in the digitized picture become quite involved. Even with today's powerful computer hardware, extensive time for the processing is required (9:445).

One way in which the computation time problem could be minimized is to allow some of the computing to be done optically before the image is sent to the computer (7:69). This is possible since many of the pattern recognition techniques currently in use rely on a multi-step process for recognition. A popular first step is to pick out all of the edges in the picture and make them brighter (9:445; 12:83). This is called edge enhancement. By doing this, the outlines of the targets are enhanced and the recognition task might be easier.

A digitized image is represented by a matrix of numbers. Each of these numbers represents a quantized version of the radiance incident on a single picture element called a pixel. An electronic pattern recognition program operates on the pixels by applying different mathematical operations to the numbers. The current state of the art in electronic edge detectors can process 512 x 512 pixel images at 25 frames per second (9:445). Even this high rate of processing slows the processing of a given image by 40 milliseconds. In the automated target recognition problem already mentioned, a missile so equipped traveling at the speed of sound would travel about 13.4 meters in this amount of time, and this is only the first step in the pattern recognition task. If done optically, this time could be significantly reduced. An optical processor could be constructed with an optical path length of one meter (15:2799). Assuming that the image to be enhanced is available to the processor, this processor could perform the edge enhancement task in less than 4 nano-seconds, or about 10 million times faster than the electronic edge enhancer. The missile in question would only travel 112 nano-meters in this time.

It is a well documented fact that when a transparency located in the front focal plane of a lens is illuminated by coherent light (such as laser light), the resulting optical field in the rear focal plane is proportional to the Fourier transform of the transmittance function of the transparency.

This process is shown in Figure 1.1 (6:87-88). The Fourier transform represents the spatial frequency content of the object which was used to record the transparency.

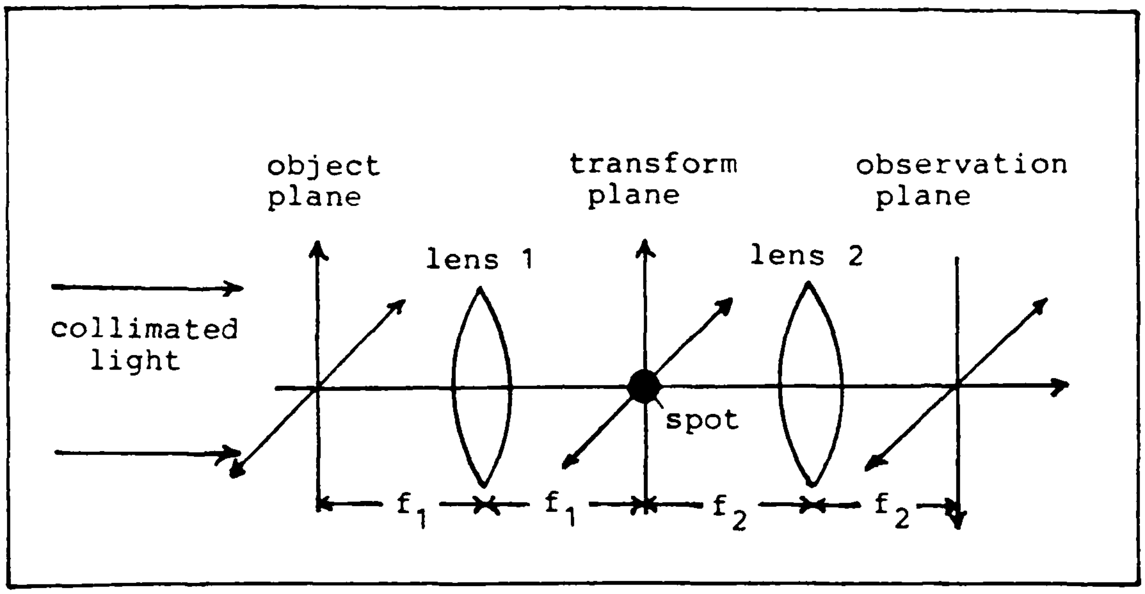

Figure 1.1. Optical edge enhancement

This Fourier transform, if passed through another lens, will produce an image of the transmittance function of the original transparency (6:10). If, however, a "small" opaque spot is put into the center of the Fourier transform plane, where "small" means the spot is small in comparison with the spatial extent of the spatial frequency spectrum, the lower spatial frequencies of the image will be filtered out. In essence, the Fourier transform can be interpreted as a two-dimensional plot of the rate at which the contrast of the transparency changes as a function of distance in the plane of the transparency. The opaque dot will, therefore,

block the the portions of the image where the contrast varied slowly with distance, leaving only the portions that varied with a higher frequency. The light passed includes the edges of the objects in the image. Therefore, the new image is essentially the outlines of the original image (7:69). Since light passes almost without delay through the lenses, the entire process of highlighting the edges of the image occurs almost instantaneously. This new image could be digitized and fed into the pattern recognition program, effectively eliminating the time delay normally associated with electronically edge enhancing the image (7:69).

This method of edge enhancement works fine in the laboratory, but little work has been done to actually test it in real world conditions. Under actual conditions, the targets of interest will probably be illuminated with incoherent light. This makes the above edge enhancement process much more difficult since the Fourier transforming properties of lenses, as explained above, assumed that the object was illuminated with monochromatic or quasimonochromatic, spatially coherent, light. One way of solving this problem is to image the target onto a spatial light modulator (SLM) which can be used to impress an image onto a laser beam for processing. An incoherently illuminated image could be imaged onto a SLM simply by viewing the image with a conventional television camera (vidicon) and driving the SLM with the output of the camera. The SLM then modulates the laser, thus providing the

coherent image needed for optical edge enhancement. The SLM used must be capable of being addressed in real time to accommodate a changing target environment.

There are several spatial light modulators available today, but most are very expensive. Currently, though, liquid crystal technology has progressed to the point where low cost liquid crystal televisions have become commercially available. Casio Inc, Magnavox, Panasonic, Radio-Shack, Sony, and Zenith, to name only a few, all market a pocket television using liquid crystal technology for under $200.00. Some of these televisions can be made to perform as spatial light modulators with only a minimum of effort (14:1380). Although they don't have the pixel resolution or the dynamic range of the more expensive SLM's they could serve well as an experimental tool to investigate the concepts discussed in this thesis.

Scope

This thesis will investigate possible applications of a low-cost liquid crystal television as a spatial light modulator. The applications of interest will be limited to possible uses in an optical pre-processor for an electronic pattern recognition system. One such application, already introduced, is the optical edge enhancement as a pre-processor. Three implementations of this application will be investigated; edge enhancement by Fourier transform spatial filtering, edge enhancement by image cancellation,

and phase only edge enhancement which was developed during this research.

It will be assumed that the enhanced images produced by the optical pre-processor, will be further processed by an electronic pattern recognition system. The exact nature and performance of the electronic pattern recognition system will not be addressed in this thesis. The applications investigated will also assume that a coherent light source (a laser) is available. The properties and physics of the coherent light source will not be addressed.

Thesis Outline

Chapter two of this thesis will present some background material on Fourier Optics and may be skipped if the reader is familiar with the subject. Chapter three is a rather involved chapter on the operation of the liquid crystal television as a spatial light modulator. It addresses the construction of the television, operation principles, modifications which had to be performed on the television so it could be used as a spatial light modulator, and its performance. Chapter four addresses the experimental configurations used throughout the thesis and chapter five the results of the experiments. The thesis will conclude with a chapter of conclusions and recommendations.

II. Background

This thesis investigates the suitability of a liquid crystal television (LCTV) for applications as a spatial light modulator (SLM) in optical pre-processors. The applications of interest will involve the use of the LCTV as a SLM within an optical processor consisting of a laser, polarizers, an assortment of lenses to image and transform the wavefront of interest, and various instruments for measuring and analyzing the resulting fields at different points in the optical processor.

This chapter will provide the background necessary to understand how the optical processor functions. The first section will address and define the Fourier transforming properties of lenses; a property of major significance in this thesis. The second section will discuss one way in which the edges of an image can be enhanced; by Fourier transform spatial filtering, and the last section addresses another method of enhancing edges, that of image cancellation. The last section also lists some of the applications of the type of optical pre-processor discussed in this thesis.

Transforming Properties of Lenses

As mentioned in the introduction, it has long been known that when a transparency located in the front focal plane of a converging lens is illuminated by coherent light (such as laser light), the resulting optical field in the rear focal plane is proportional to the Fourier transform of the transmittance function of the transparency (6:87-88). A mathematical description of this Fourier transforming property will be presented here without proof, but first some definitions are in order. The Fourier transforms of interest in this application are two-dimensional Fourier transforms. The mathematical representation of the Fourier transform which will be used is given by

$$U_f(f_x,f_y) = \iint_{-\infty}^{\infty} t_o(x,y)\exp[-j2\pi(f_x x + f_y y)]dxdy \qquad (2.1)$$

where $U_f(f_x, f_y)$ is the Fourier transform of the field $t_o(x,y)$. The arguments f_x and f_y are the coordinate axes of the Fourier transform and represent spatial frequencies in the x-direction and y-direction respectively (6:49). This field $t_o(x,y)$, in the applications here will represent the transmittance of the transparency to be transformed.

Lenses can be used to find information about the Fourier transform of a field or transparency in two different ways; with the transparency in front of the lens and with the transparency behind the lens. Only the case of the transparency before the lens will be discussed here. It

will be assumed that the light incident upon the transparency is collimated, monochromatic, and coherent. This incident light will be referred to as a normally incident, uniform amplitude plane wave in consistency with the standard literature. If the transparency is located in front of the lens, the resulting field at the rear focal point of the lens is given by

$$U_f(x_f, y_f) = [A/(j\lambda f)]\exp\{[jk/(2f)](1 - d/f)(x_f^2 + y_f^2)\}$$
$$\iint_{-\infty}^{\infty} t_o(x_o,y_o)\exp\{[-j2\pi/(\lambda f)](x_o x_f + y_o y_f)\}dx_o dy_o \qquad (2.2)$$

where

A = a constant scaling factor
d = distance in front of the lens
f = the focal length of the lens
λ = the wavelength of the light used

In this equation the x_o and y_o are the coordinate axes in the plane of the transparency and x_f and y_f are the coordinate axes in the plane of the rear focal plane of the lens. It is easily seen that if the change of variables $f_x = x_f/\lambda f$ and $f_y = y_f/\lambda f$ are made then the integral portion of this equation becomes the Fourier transform of the transmittance of the transparency. If, in addition, the transparency is placed in the front focal plane of the lens then d = f and the exponent within the first complex exponential term of equation 2.2 is zero and the field is the exact Fourier transform of the transmittance of the transparency (6:86,87). It is this property that enables edge enhancement of an image by simply filtering the

edge enhancement of an image by simply filtering the frequency content of the transparency's transmittance function which is formed in the back focal plane of the lens.

Optical Edge Enhancement

By now, the idea of filtering the low-frequency portion of an image's Fourier transform in order to obtain its edges should be pretty clear. To summarize, the steps involved will be listed. The image is first made into a transparency which is placed in the front focal plane of a converging lens. The transparency is then illuminated by a normally incident uniform amplitude plane wave. This creates a field in the rear focal plane which is the Fourier transform of the transmittance of the transparency. An opaque spot is placed in the Fourier transform plane centered on the optical axis of the lens. This spot blocks the low frequencies allowing the higher frequencies to pass. These higher frequencies contain the edges of the image. A second lens is placed so that the Fourier transform plane of the first lens is in the front focal plane of the second lens. This results in another Fourier transform of the filtered Fourier transform which is the edges of the original image.

The areas between the edges in the original image vary slowly in contrast and, therefore, consist of low spatial frequencies and have been filtered out. If the image

obtained at the rear focal plane of the second lens were to be recombined with the original image, the areas between the edges would be filled in again, but now the edges from the original image would be multiplied by the energy from the edges in the processed image resulting in the edges being emphasized with respect to the rest of the original image. This could be accomplished by placing a beam splitter in the laser beam before the first lens and splitting the beam into two portions. One of the two beams would then go on through the lenses discussed so far, while the other one could be reflected off from mirrors around the lens set-up. This reflected light is the original image which could be aligned with the image in the rear focal plane of the second lens, thus giving the emphasized image.

The filtered Fourier transform is actually the product of the Fourier transform of the transmittance of the transparency and the transmittance of the filter (opaque dot). Once this filtered Fourier transform is Fourier transformed again, the resulting image is the convolution of the Fourier transform of the transmittance of the filter with the original image. This assumes that the size of the lenses are sufficiently large that the entire transmittance of the transparency passes through the first lens and that the highest spatial frequency of interest in the Fourier transform passes the second lens. By making this assumption, the apertures of the lenses can be ignored when computing the Fourier transforms.

Since there is a convolution of the image with the filter, the shape of the filter becomes important. For an example of this convolution it will be assumed that the original image is a rectangular function given by $\mathrm{rect}(x_o/\tau)$ and that the filter is another rectangular function, $1 - \mathrm{rect}(x_f/\alpha)$ where τ and α are, respectively, the widths of the rect functions. These are shown in Figure 2.1. The Fourier transform of the first rect is $\tau\mathrm{sinc}(\tau f_x)$. This sinc function is multiplied by the filter resulting in $\tau\mathrm{sinc}(\tau f_x)[1 - \mathrm{rect}(x_f/\alpha)]$. After taking the Fourier transform again with the second lens, the resulting field is $\mathrm{rect}(x_i/\tau) * [\delta(x_i) - \alpha\mathrm{sinc}(\alpha x_i)]$ as shown in Figure 2.2.

The figure shows that there is a ringing effect in the enhanced image due to the side lobes of the transform of the filter. These ringing effects can be minimized if a filter is chosen that has a linear taper or gaussian taper rather than a sharp cut-off as in the case of the rect function. The transform of a gaussian is another gaussian, therefore, there are no side lobes to convolve with the original image to form the ringing. Notice, also that the resulting

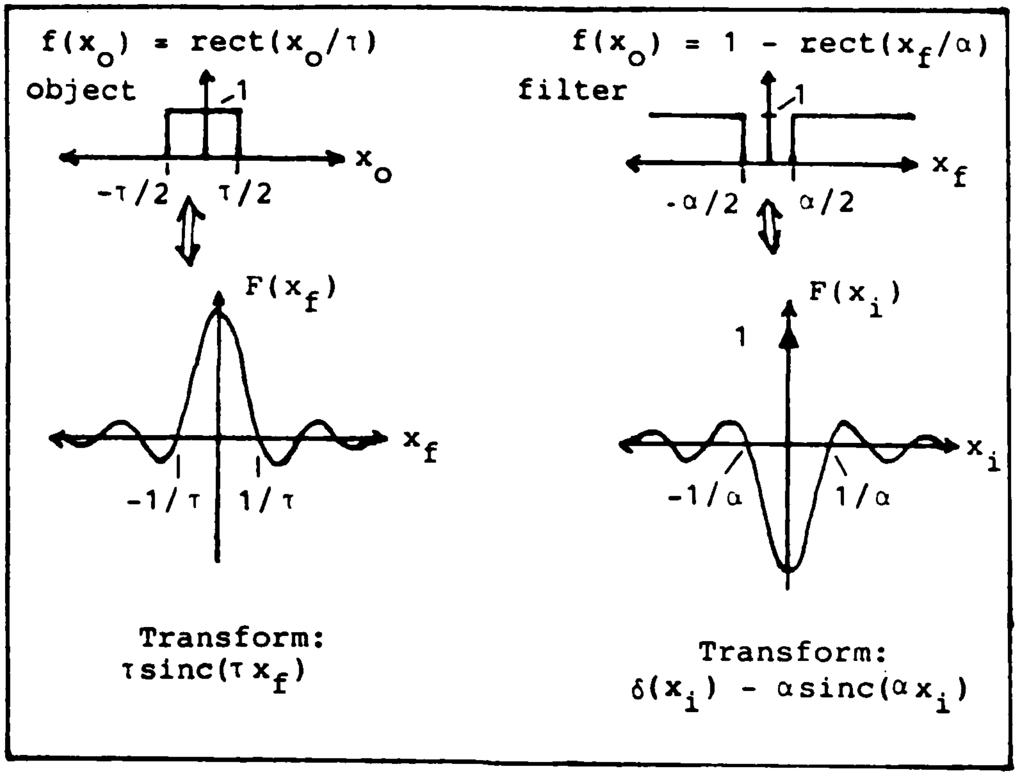

Figure 2.1. Original object, filter and their Fourier transforms.

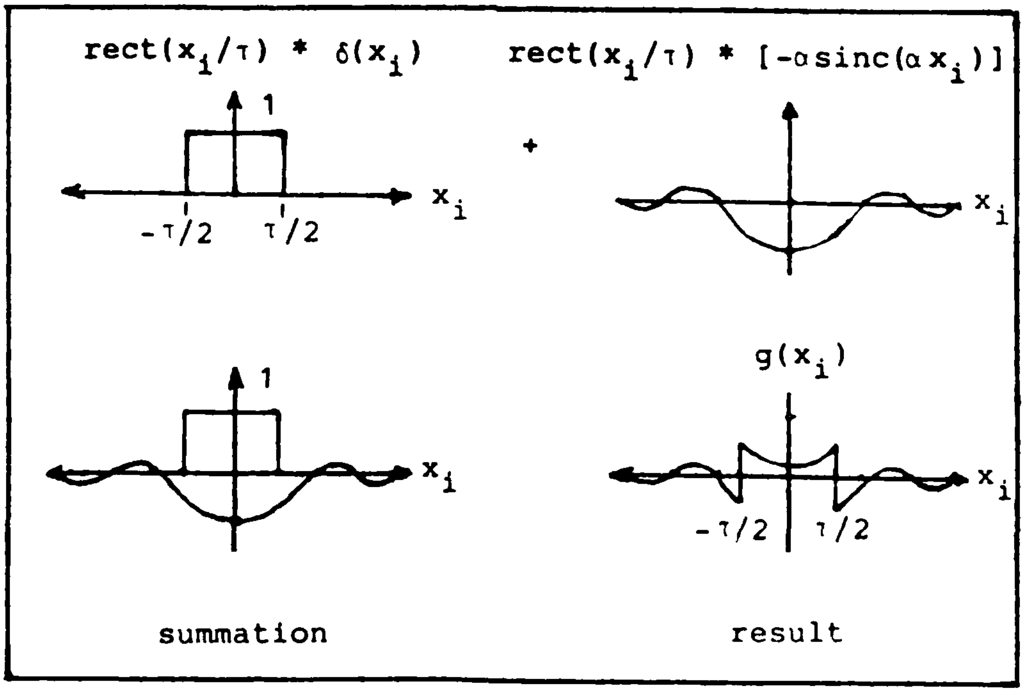

Figure 2.2. Convolution of the object with the transform of the filter

enhanced image has a phase shift of 180° at the edge of the image. The 180° phase shift will be present no matter what the object is in the front plane of the processor. If a perfect rect function were used and all of the higher spatial frequencies had passed through the optical system, this phase shift would be perfectly vertical. Since the phase information cannot be detected by the human eye or by film, this vertical phase shift would not be visible. In practice, though, there is no such thing as a perfect rect function and all optical processors have finite apertures. The finite aperture will filter out some of the high frequencies in the transform of the rect function and the resulting image after the second Fourier transform will not be a perfect rect function. All this results in some slope to the phase shift line and it will appear as a thin black line in the image of the enhanced rect function as shown in Figure 2.3.

An actual example of the convolution discussed is shown in Figure 2.4. The figure shows both the original image and the enhanced image. The filter in this example was a small circular spot which would exhibit a rectangular cross section. Notice the ringing effect as well as the thin black line at the edges of the image.

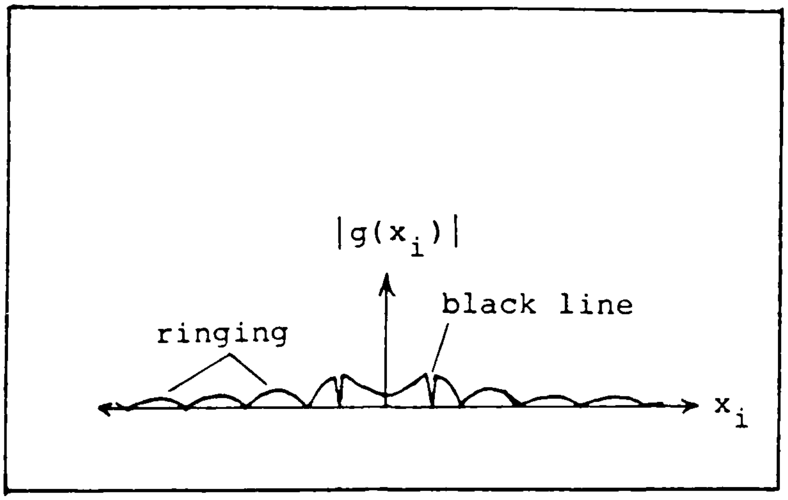

Figure 2.3. Magnitude of the enhanced rect function

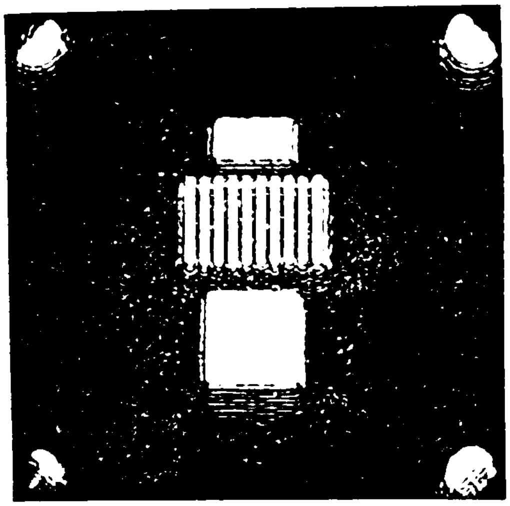

Original object

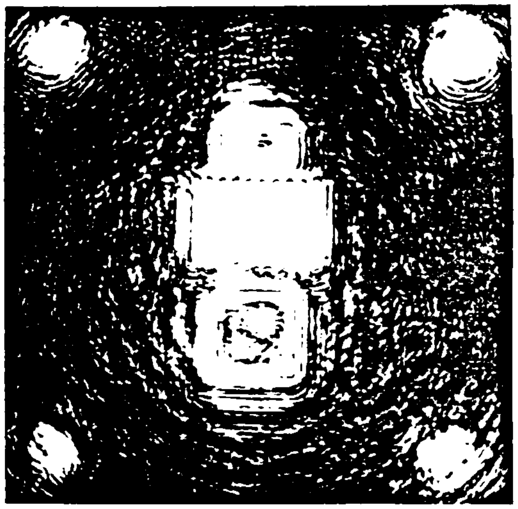

Enhanced image

Figure 2.4. Example of optical edge enhancement

Image cancellation

There is another way in which images could be edge enhanced optically other than high-pass filtering of the Fourier Transform. This alternate method uses image

cancellation or, more accurately, image cancellation through multiplication. Conceptually, the method is very simple. In this method, instead of making one transparency of the image, two are made. The second transparency, though, is the negative of the first (in the photographic sense). The first transparency is then placed in the front focal plane of the double Fourier transforming processor previously described. The second transparency is placed in the back focal plane of the second Fourier transform lens so that the image of the first transparency is projected onto the second transparency. The second transparency must be placed upside down and flipped about the vertical axis since the image of the first transparency is upside down and flipped about the vertical axis after passing through the processor. The Fourier transform of the first transparency is then spatial filtered, filtering out the higher spatial frequencies so that the image of the first transparency is blurred in the plane of the second transparency.

To understand how this results in edge enhancement, assume for the moment, that the first transparency was imaged exactly (not blurred), and that the image was binary, consisting only of perfectly clear portions and perfectly black portions. The field immediately behind the second transparency is the product of the field and the transmittance of the second transparency, or, effectively, the product of the transmittances of the two transparencies. Since the transmittance of the second transparency is the

negative of the first, the transmittance of regions which were bright (near unity transmittance) on the first transparency would be black (very small transmittance) on the second and visa versa. The resulting field would, therefore, be a very small transmittance multiplied by a larger one over the entire screen area. Ideally, the transmittance of the dark regions would be zero making the resulting image identically equal to zero, but in reality these black regions may have a finite, though small, transmittance. The resulting field is, therefore, non-zero, but very small and uniform in intensity. This result, obviously, depends a great deal on having the second transparency exactly lined up (registered) with the field from the first. It also depends on having the two transparencies exact negatives of each other with any imperfections being uniform over the area of the transparencies. If, however, the image of the first transparency were low-pass filtered before it impinged on the second transparency, the edges of the first image would be blurred. The result would be a gray area of the field multiplied by the clear portion of the edge on the second transparency yielding a gray line behind the transparency where the edge had been. The lower frequency portions of the image which were not filtered out would cancel out as previously mentioned. The final result yields an image containing only the edges of the original image.

This technique breaks down when the original image is composed of a variety of different gray levels. Where the first transparency had been some shade of gray, the second would be the inverse, or another shade of gray. The product of the two shades of gray is just another shade of gray and not zero. The overall resulting image, would be an image which consisted only of those areas of the original image which were gray. If the original image was entirely a mixture of gray levels, the resulting image would be another mixture of gray levels where the edges may not be enhanced at all. This will be demonstrated in Chapter 5. One way to solve this problem would be to quantize the gray-level image to a binary image so that any gray level above a given threshold would be converted to clear and any gray level below the threshold converted to black. This quantizing would have to be done before making the transparencies. The end result is the same as in the binary case already discussed.

Applications

The techniques discussed here would be very useful in a pattern recognition application as discussed in the introduction. An optical processor consisting of an edge enhancer used as a pre-processor for an electronic pattern recognition system, could significantly increase the speed at which the overall system could function. These types of pre-processors, though, in a real world example, would have

to be able to deal with a dynamic input image. Take the missile seeker example. As the missile flies toward its target, the image that the missile's optical sensor presents to the processor would be continually changing. It would, therefore, be impractical to attempt to make transparencies of the input scene for use in the coherent processor.

The easiest way to solve this problem is to use a Spatial Light Modulator (SLM) as discussed in the introduction. In the introduction, the use of the spatial light modulator was to convert the incoherent input scene to a coherent one, but the same solution will work for allowing the input scene to be dynamic. This, of course, requires that the SLM have enough pixels to provide sufficient resolution for accurate identification, be capable of being dynamically addressed and at a high enough rate so that the advantage of using the optical pre-processor is not lost. Such a SLM would make the optical pre-processors discussed here viable alternatives to all electronic pattern recognition systems.

Conclusions

In this chapter the Fourier transforming properties of lenses were briefly discussed as well as how these properties could be used to form a generic optical Fourier transform processor. A couple example applications of such a processor were discussed; the edge enhancement through spatial filtering and edge enhancement through image

cancellation as well as how these applications could be useful as optical pre-processors for a pattern recognition system. These applications brought out the need for replacing the transparencies discussed in this chapter with a more dynamic medium; the spatial light modulator.

Such SLM's exist, as mentioned earlier, but they are very expensive. The rest of this thesis will address how a low-cost Liquid Crystal Television (LCTV) can be modified to operate as a SLM. It will then be used to investigate the performance of such a mass produced product in an optical processor. The technology used in building the LCTV may well be able to reduce the cost involved in producing SLM's for implementing optical pre-processors for military and industrial use. The next chapter will discuss the required modifications to the LCTV as well as the principles of its operation as a SLM.

III. Operation of the Liquid Crystal Television

In this chapter, properties of the liquid crystal television (LCTV) are characterized. In the first section, the construction of the liquid crystal display will be discussed. This is followed in the second section by the LCTV's operation principles. The third section addresses the modifications required to use the LCTV as a spatial light modulator (SLM). In the fourth through the sixth sections the performance of the SLM will be discussed.

The LCTV used was the Realistic model 16-153 black and white TV. It is readily available commercially at a cost of less than 100 dollars. This model is especially appropriate for the applications of interest since it comes equipped with an external power supply, a video input jack, and an external rf input jack. The video input jack allows the LCTV to be addressed directly by a computer or a television camera.

Display Construction

The TV has a 2.7 inch diagonal measure screen and a resolution of 120 vertical pixels by 140 horizontal pixels. The liquid crystal display is constructed of two parallel pieces of glass separated by 0.3 mil (7.62 microns). The 0.3 mil gap is filled with nematic liquid crystal material.

There is also a polarizer both in front of and behind the display. A cross section of the display construction is shown in Figure 3.1. One of the two glass plates has 120 horizontal wires imbedded in it. These act as the horizontal drive lines for the pixels. The other plate of glass has the 140 vertical drive lines imbedded in it. The intersection of two of these drive lines forms a pixel (11:12). In order to avoid confusion, the horizontal drive lines will be referred to as line electrodes and the vertical drive lines will be referred to as segment electrodes.

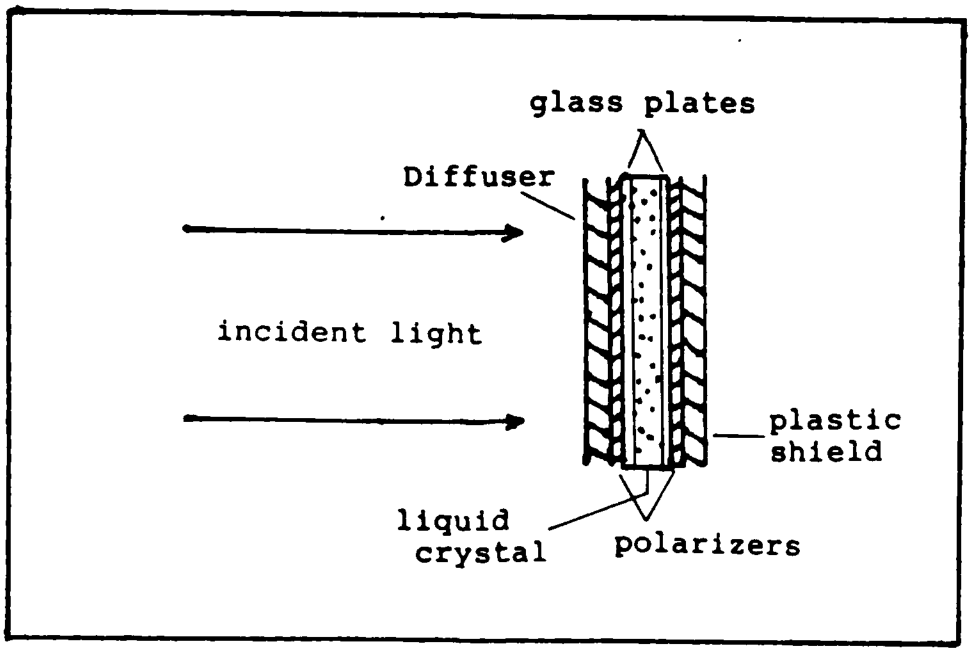

Figure 3.1. Construction of the LCTV display

Line and segment electrodes can been seen in Figure 3.2, a photo of an enlarged portion of the screen. In order to make these pixels uniformly shaped (rectangular), there

appears to be transparent flat electrodes deposited on the glass over the drive wires as shown in Figure 3.3. These flat electrodes are in contact with the drive wires and allow the electric charge to affect the liquid crystal material uniformly over the area of the electrodes. Where the drive lines on opposite plates of glass intersect, the intersection of the flat electrodes forms a rectangle as shown in the figure. Each of these rectangles are pixels. This pixel structure can be seen in Figure 3.4; notice the lighter lines between the drive lines. These are the boundaries of a pixel. This photo was taken with the TV turned on with a black screen as the input, while the photo in Figure 3.2 was taken with the TV off so that the electrodes did not show up.

Figure 3.2. LCTV drive lines.

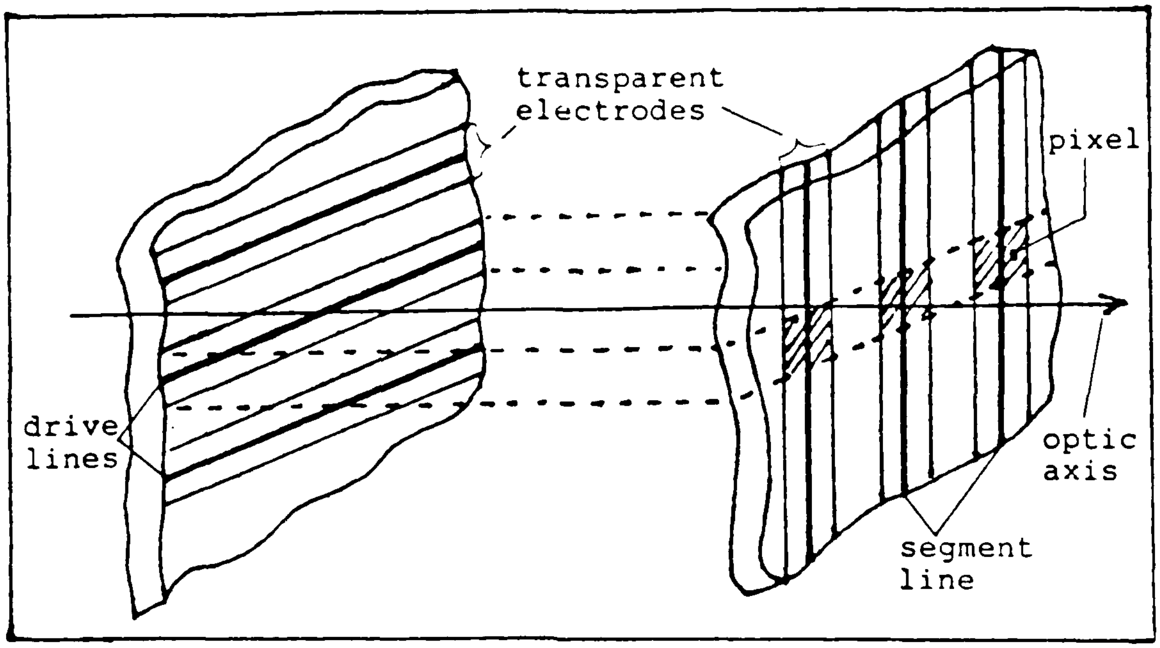

Figure 3.3 Transparent electrodes deposited over the drive lines on each plate of glass

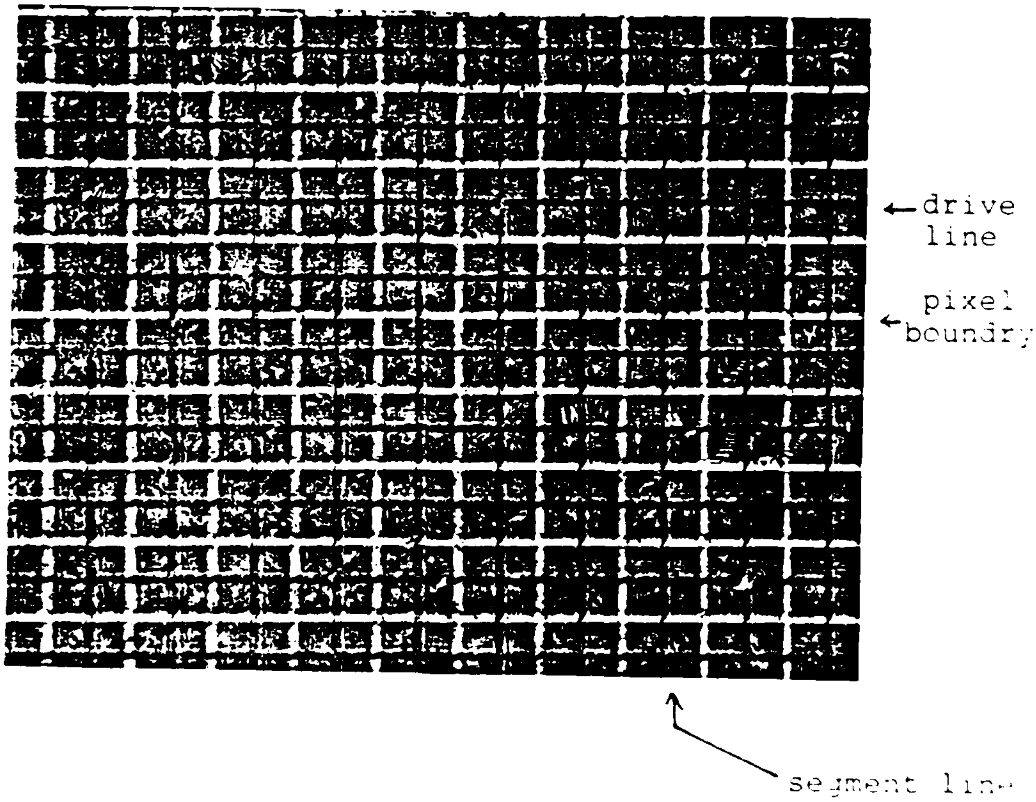

Figure 3.4 LCTV pixel structure

Basic Operation Principles

The display modulates light passing through it by polarization rotation. The first polarizer on the front (left side of Fig 3.1) of the display ensures that the light entering the nematic liquid crystal material is linearly polarized at the appropriate angle. The molecules of the nematic liquid crystal are twisted about 90 degrees when there is no electric potential between the drive lines. This twist is shown in Figure 3.5a (1:125), it is accomplished by coating the inside of each plate of glass with a directing material, such as lecithin, which causes the molecules of the liquid crystal to align themselves with the director. The directing material is applied to each plate of glass in a specified direction, with the direction on the two opposite plates perpendicular to each other. As long as the entering light is polarized in the same direction as the molecules against the first plate of glass, the polarization of the light will follow the rotation of the molecules as it passes through the material. This results in outgoing light that is linearly polarized, but with its plane of polarization rotated 90° about the optic axis with respect to the entering light. This light is blocked by the second polarizer which is oriented in the same direction as the first one and acts as a polarization analyzer (11:12; 1:126). The twist effect will occur whenever there are sufficient molecules in the spiral, or in other words, when the nematic material is thick enough. The

thickness required for frequencies above a given wavelength is known as Mauguin's condition. For thicknesses above 10 microns Mauguin's condition is satisfied for all wavelengths in the visible range, (wavelengths below about 1 Micron). In this case, though, the thickness is only 7.62 microns. Since the wavelengths for which Mauguin's condition are satisfied is directly proportional to the thickness of the nematic material, the thickness of 7.62 microns will satisfy Mauguin's condition for wavelengths below about 0.76 microns (1:126). This range of light is still suitable for operation as a television and for the application of spatially modulating a laser. A helium-neon laser, for example, has a wavelength of 0.6328 microns.

Once a pixel is selected, an electric potential is applied between the two electrodes on each glass plate. The resulting electric field causes the molecules in the center of the nematic material to align themselves with the electric field as shown in Figure 3.5b (1:125). This realignment leaves only the molecules on the ends of the spiral to affect the polarization of the light. These regions are too thin to satisfy Mauguin's condition and the light passes unchanged (1:126). This realignment, or deformation begins to occur for voltages above the deformation threshold. The voltage must be considerably above the deformation threshold before enough molecules are realigned so that Mauguin's condition is not satisfied. The actual voltage required for this condition will be referred

to as the optical threshold. The difference between the deformation threshold and the optical threshold varies with the frequency of light being passed as well as the structure and composition of the liquid crystal cell (1:127). For this display the deformation threshold is about 1.6 volts and the optical threshold is more than six times this voltage (11:12) . The optical performance will be discussed in more detail later.

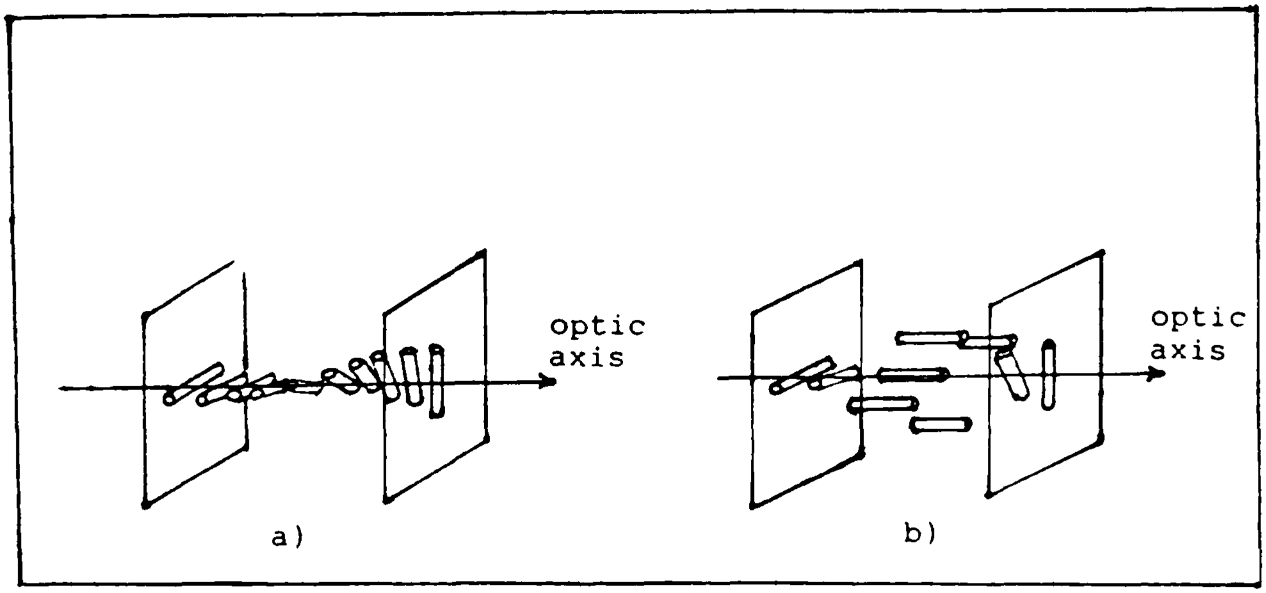

Figure 3.5. Twisted nematic liquid crystals, a) with no electric potential, b) with a large electric potential.

When the LCTV is in operation, the line (horizontal) electrodes are driven by a +13.5 volt pulse, 133 microseconds in duration, every 1/60 second. The segment (vertical) electrodes are driven by two different drivers, one for the top half of the screen, the other for the bottom

half of the screen. When the line electrodes in the top half of the screen are being addressed, the segment electrodes in the top half of the screen are all being driven simultaneously. Similarly when the line electrodes on the bottom half of the screen are being addressed, the segment electrodes in the bottom half of the screen are all being driven. The segment electrodes are driven by a pulse whose amplitude is either positive or negative. If the selected pixel is to be bright, the segment electrode is driven by a negative voltage. If the pixel is to be dark, it is driven by the positive voltage. This yields a greater electric potential difference between the segment electrode and line electrode when the selected pixel is to be made bright. The gray level of the pixel, or brightness, is determined by the width of this pulse (11:11). Recall, that the polarization of the light is not affected when there is a high electric potential across the pixel, and that otherwise the polarization is rotated 90°. With parallel polarizers on each side of the display, the light passing through the bright pixel will pass the second polarizer while the light passing through a dark pixel will be rotated 90° and will be blocked by the second polarizer. If the width of the driving pulse is shortened, the pixel will be bright for a shorter time. The human eye will average the resulting light and, compared with a pixel driven with a longer pulse, will appear dimmer or gray. The human eye can differentiate between individual pulses of a pulsed light

source only until the frequency of the pulses reaches a certain frequency at which the light will appear to be on steadily. The upper limit of this frequency varies with the intensity of the light and the rise time of the pulses, but the extreme upper limit is about 40 Hz (3:396-397). The LCTV pulses each pixel at a 60 Hz rate and the pulses, therefore, are not seen by the viewer.

The brightness control on the TV selects the bias voltage on the segment electrode pulses. The peak-to-peak voltage swing on the segment pulses is 3.6 volts. The brightness control allows the center of this swing to vary so that at maximum brightness the negative pulse is near zero and the positive pulse is near 3.6 volts. Similarly, at the other extreme, the positive voltage is near zero while the negative voltage is near -3.6 volts. The net voltage difference between the line electrode and segment electrode for a "dark" pixel, with the brightness turned completely down is still 9.9 volts, but this voltage level produces a negligible change in the rotating properties of the liquid crystal.

Modifications of LCTV

Before the LCTV could be used as a spatial light modulator, it had to be modified from its television configuration. When functioning as a television, the liquid crystal display is hinged and can only open about 60 degrees. The light is allowed to enter through the display

and then is viewed in a mirror as shown in Figure 3.6. This hinge had to be taken apart so that it could be opened 90 degrees.

The original polarizers on the TV were glued to the glass plates which contained the nematic liquid crystal. In the normal viewing configuration, the incident light first passed through a diffuser before the first polarizer and protecting the second polarizer, there was a clear plastic plate. This diffuser and plastic plate were removed. The original polarizers were also removed so that higher quality ones, which could be reoriented at will, could be used.

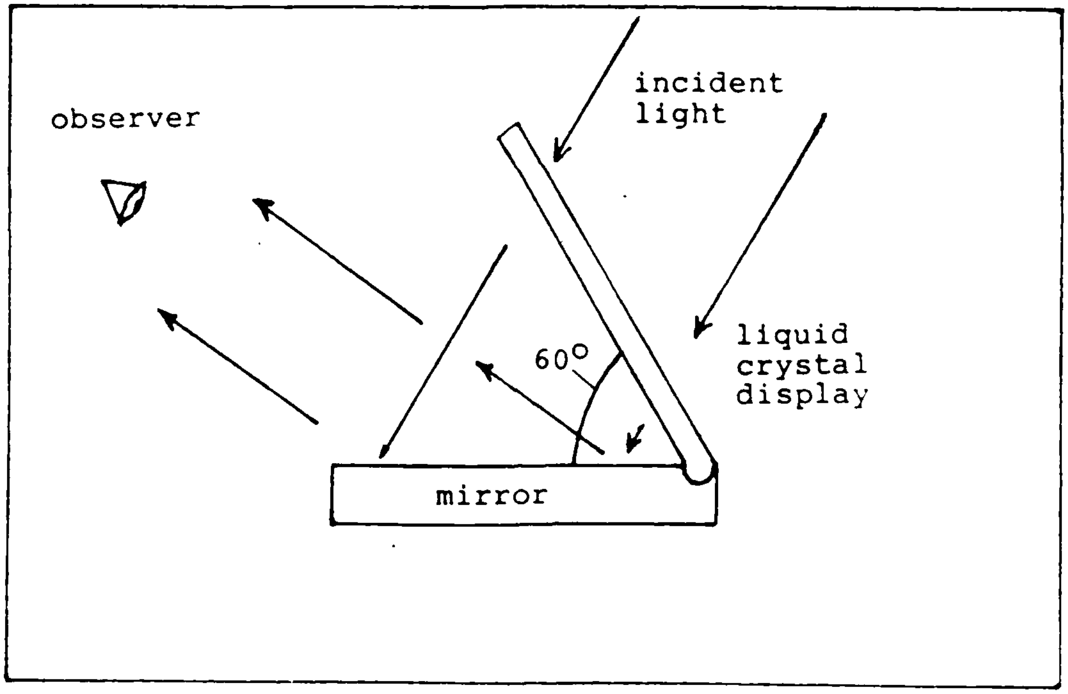

Figure 3.6. Normal viewing configuration for the LCTV as a television.

The glass plates of the display are of poor optical quality and provide considerable distortion to the traversing laser beam. The imperfections in the glass

plates for one of the LCTVs used were removed by immersing the LCTV in a liquid gate (4:246). The gate was made up of a cell constructed of optical flats filled with microscope slide immersion oil. The oil used was non-drying immersion oil for microscopy, formula: code 1248 type A, produced by R. P. Cargille Laboratories Inc. The improvements in the optical quality of the display were apparent from viewing the Fourier transform of the display. Without the liquid gate, the Fourier transform of the display appeared 'smeared' due to the convolution of the transform of the imperfections in the glass with the periodic nature of the drive lines. A photo of the Fourier transform of the display without the liquid gate is shown in Figure 3.7. Figure 3.8 shows the central spot of the Fourier transform both with and without the liquid gate. Both photos were taken with the televisions turned off. Notice, also, that the photo in Figure 3.7 shows the periodic nature of the drive lines.

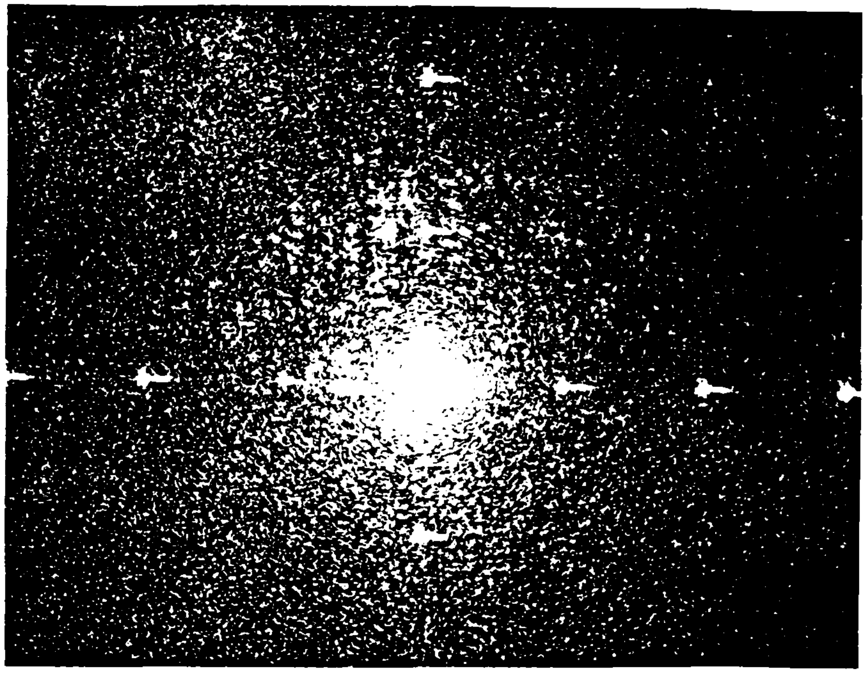

Figure 3.7. Fourier transform of the LCTV without the liquid gate.

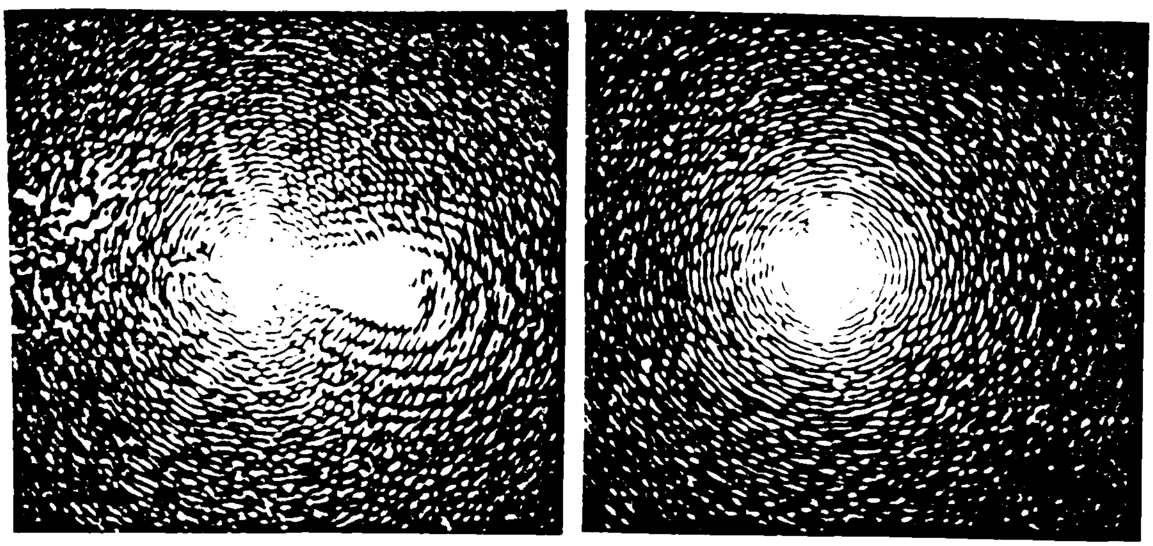

a) b)

Figure 3.8. Central spot of the Fourier transform of the LCTV a) without the liquid gate, b) with the gate.

With the television turned on, the Fourier transform is altered by the introduction of the pixel boundaries. When the LCTV was turned off the cross section of the display could be modeled by: $\text{rect}(x/\tau) * (1/T)\text{comb}(x/T)$ where τ is the transmitting distance between the drive lines. This assumes that a coordinate system is chosen with axes at the mid-point between two adjacent drive lines, and that $\text{rect}(x/\tau)$ represents the distance between the drive lines. T is the distance between the centers of the rect functions. Due to the finite width of the drive lines, T will be sightly larger than τ. The Fourier transform of this is $\tau\text{sinc}(\tau x_f)\cdot\text{comb}(Tx_f)$ as shown in Figure 3.9. With the LCTV turned on, the transmittance changes due to the boundaries of the pixels. If the polarizers are adjusted properly the boundaries appear darker than the pixels and the original rect function changes to: $\text{rect}(x/\tau) - B\cdot\text{rect}(x/\alpha)$ where α is the width of the boundary between two adjacent pixels (The white lines between the drive lines in Figure 3.4), and B is the fraction of the height of the first rect function that the second rect function occupies. This new function must also be convolved with the comb function to represent the periodic nature of the display. The Fourier transform of this new function is $\tau\text{sinc}(\tau x_f)\cdot\text{comb}(Tx_f) - B\alpha\text{sinc}(\alpha x_f)\cdot\text{comb}(Tx_f)$ as shown in Figure 3.10.

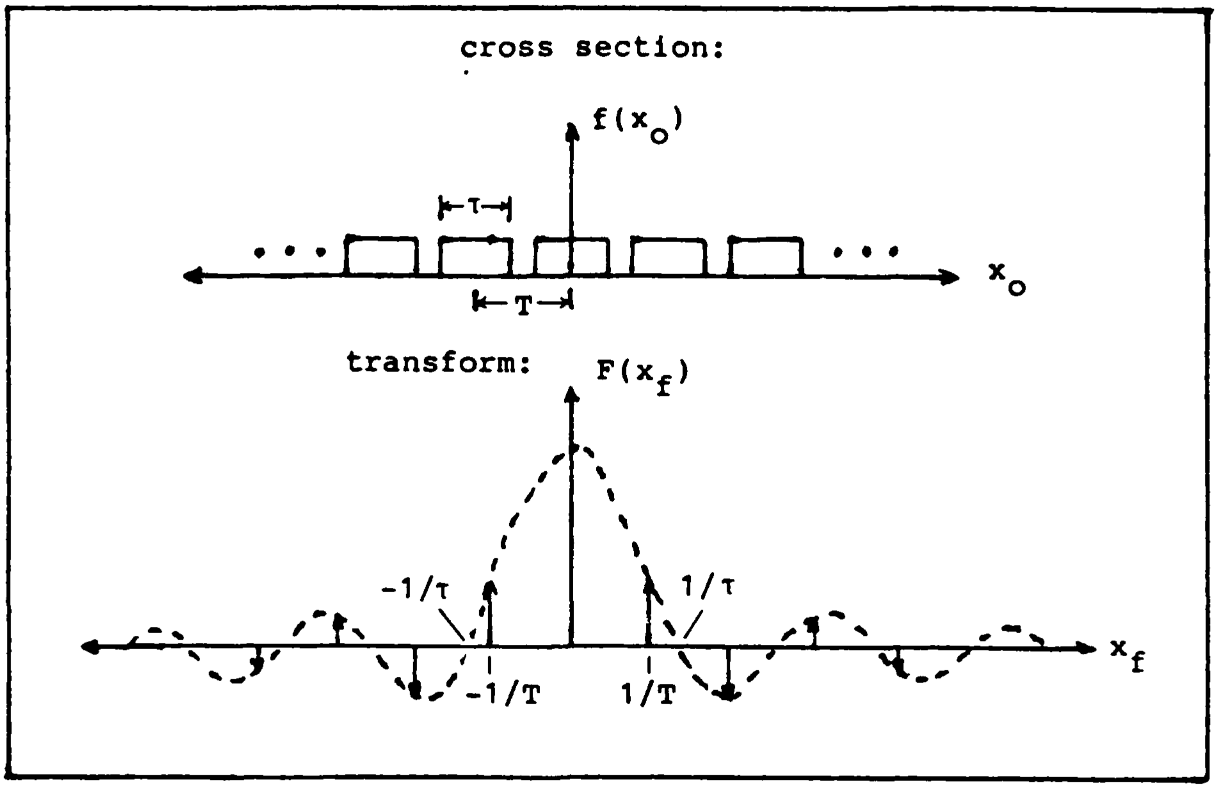

Figure 3.9. Cross section of the LCTV display and its Fourier transform with the power off

The width of the pixel boundary, α, is much smaller than width of the pixel, τ, and the transform of the rect of width α is, therefore, much wider than the transform of the rect of width τ. The pixel boundaries, though, occur with the same interval T, so both sinc functions will be multiplied by a comb function with period 1/T. Notice that in this case every other impulse of the second comb function interferes destructively with those of the first. If the polarizers are adjusted properly, the pixel boundaries appear black and the value of B approaches one. In this case, the two comb functions interfere to the point where every other impulse disappears and the resulting period of

the Fourier transform is cut in half. This should make intuitive sense, since the black pixel boundaries blocking the light effectively double the spatial frequency of the LCTV display and, hence, halve the spatial frequency of the Fourier transform. Figure 3.11 shows a photograph of the modified Fourier transform.

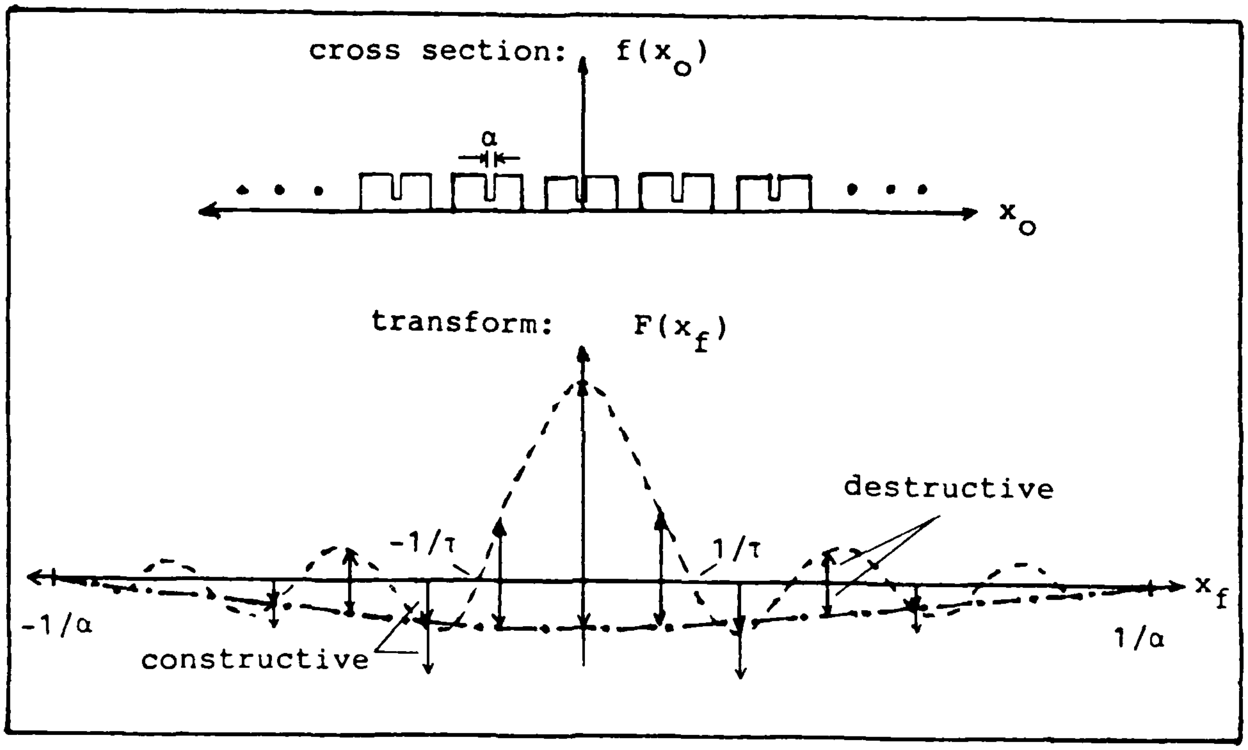

Figure 3.10. Cross section of the LCTV display and its Fourier transform with the power on

(a)

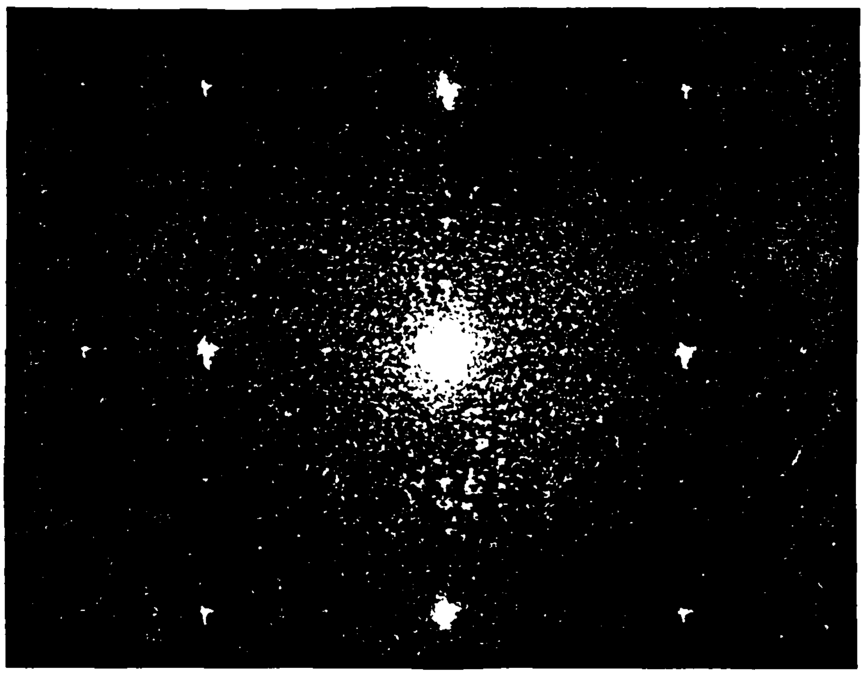

(b)

Figure 3.11. Fourier transform of the LCTV a) with the power off, b) with the power on and pixel boundaries black.

Input Polarization

The angle of polarization of the incident light is important in obtaining the best performance of the LCTV. The twisted nematic liquid crystal will effectively rotate the polarization of the incident light, retaining the linearly polarized nature of the light, as long as the polarization of the incident light is aligned with or perpendicular to the orientation of the molecules adjacent to the input glass. If the plane of polarization of the light entering the nematic liquid is not aligned with, or perpendicular to, the molecules adjacent to the input glass, then the exiting light will be elliptically polarized. Since the analyzer can only block the component of the light polarized in the direction perpendicular to its orientation more light will pass the analyzer. This elliptical polarization, will drastically reduce the performance of the display since a "dark" screen (one in which none of the pixel are bright) will not be as dark as it could be and the dynamic range of the display will be much smaller (1:126).

The elliptical polarization is a result of the birefringence of the liquid crystal material. In other words, the liquid crystal material delays the light passing through it by different amounts depending on the polarization of the light. The liquid crystal material offers the least delay to incident light polarized in a particular direction. This direction will be referred to as the fast axis. Perpendicular to the fast axis is the slow

axis. Incident light polarized in the direction of the slow axis is delayed the most. If the incident light is linearly polarized exactly in the direction of the fast, or slow, axis so that there is no component in the direction of the other axis, then the exiting light will also be linearly polarized. If, however, the polarization of the incident light is not exactly on the fast or slow axis then a component in the direction of the other axis is delayed a different amount. This results in the exiting light being elliptically polarized with the major axis of the ellipse being the fast or slow axis of the material, which-ever was closest to the polarization of the incident light.

The optimum angle for the polarization of the incident light was found to vary with the position of the brightness control. As the brightness control is turned up from the minimum setting, the electric potential across the gap rises from the minimum of 9.9 volts (for a dark screen) and causes more of a deformation of the twist structure of the liquid crystal. Although there are still enough molecules in the spiral structure to cause most of the light to rotate, the deformation of the twist structure apparently results in a change in the birefringence so that the fast and slow axes rotate slightly. This causes elliptical polarization of the exiting light since the incident light is no longer exactly aligned with the liquid crystal axes. As mentioned earlier, this results in more light passing the analyzer. For a dark screen, the amount of light which passes the analyzer

increases rapidly as the brightness voltage is increased. The plane of polarization of the input light must, therefore, also be rotated to realign with one of the axes. The deformation also allows some of the light to pass without being rotated the full 90° resulting in light that is not aligned with the major axis of the ellipse. This off axis light cannot be completely removed by adjusting the polarization of the incident light. The analyzer which is normal to the major axis of the ellipse also will not completely block the off axis light. This causes a "dark" screen to appear brighter than it had with the brightness control at the minimum.

With a brightness voltage setting of about 75%, the optimum input polarization is 16 degrees from what it was at the minimum brightness setting. The 75% brightness setting was found to give the best contrast for viewing, but did not give as black a dark screen as did the minimum setting. The brighter dark screen was compensated for by a brighter "bright" screen. Above the 75% setting the advantage of the brighter "bright" screen over the brighter "dark" screen diminished. The change in the required input polarization, the analyzer orientation, and the dynamic range of the LCTV as a function of the brightness setting is shown in Table I. The column labeled Brightness voltage in the table is the voltage drop across the potentiometer which controls the brightness, it is not the voltage across the liquid crystal. The brightness control was at the maximum position when

there was a 1.6 volt drop and at its minimum when there was a 0.0 volt drop.

Table I
Optimum polarization angles as a function of the voltage drop across the brightness control potentiometer

Brightness voltage	Input polarization (degrees)	Analyzer orientation (degrees)	Dynamic range (dB)
1.6	26	49	3.3
1.5	32	50	7.4
1.4	37	51	7.0
1.3	40	50	9.0
1.2	41	47	11.8
1.1	43	46	11.5
1.0	45	46	11.5
0.9	47	44	11.5
0.8	48	42	10.2
0.7	49	40	10.0
0.6	51	37	10.6
0.5	52	36	10.4
0.4	53	35	10.7
0.3	54	34	10.9
0.2	55	33	10.3
0.1	55	33	9.5
0.0	56	32	10.4

Dynamic Range

The current state of the art in spatial light modulators can provide for up to 30 dB of dynamic range (8:251), but only at a high cost (usually thousands of dollars). By contrast, the dynamic range of the LCTV was found to be only about 10 to 11 dB (see Table I). While this does not sound very good, this 10 dB did provide enough contrast to be easily seen and measured.

The dynamic range figures shown in Table I were found by measuring the brightness level of a "bright" pixel on a

video analyzer and comparing it to the level of a "dark" pixel. The only problem with this measurement is that the video analyzer integrates the intensity over time. The individual pixels, however, are not turned on all of the time. As mentioned earlier, the line electrode is scanned at a rate of 1/60 of a second and is pulsed with a 13.5 volt pulse only 133 microseconds long. Therefore, the pixel is only being excited for a small portion of the 1/60 second interval. During the rest of the interval, the pixel is recovering and the transmitted light intensity is diminishing.

The time response of a pixel was measured by magnifying the display such that a single pixel could be sensed by a photodetector. The results are shown in Figure 3.12 for both minimum and maximum brightness voltage. These plots show the intensity of the light passing the analyzer. If the intensity of the transmitted light were to be measured only at the peak of the time interval, rather than averaged over the entire interval, the dynamic range would probably increase.

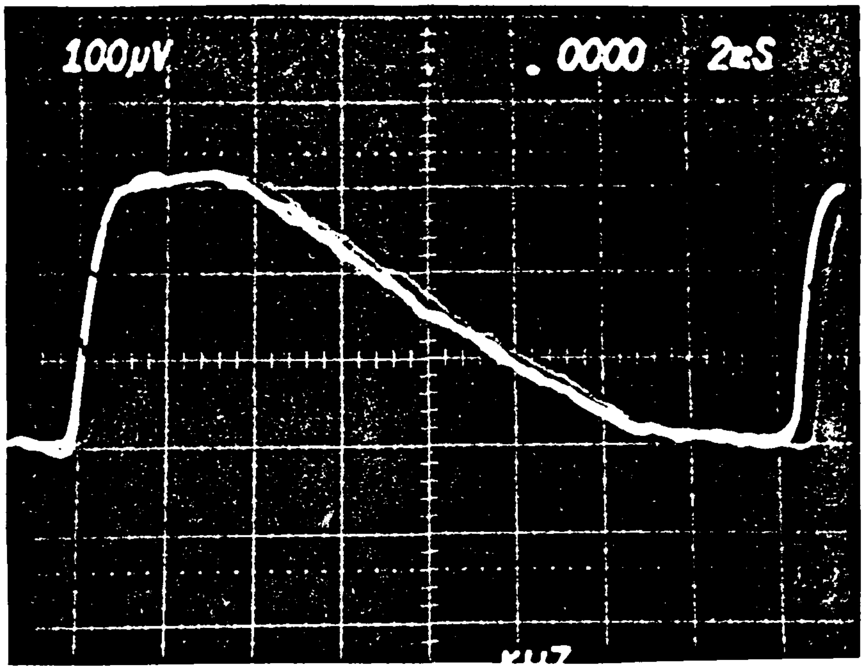

(a)

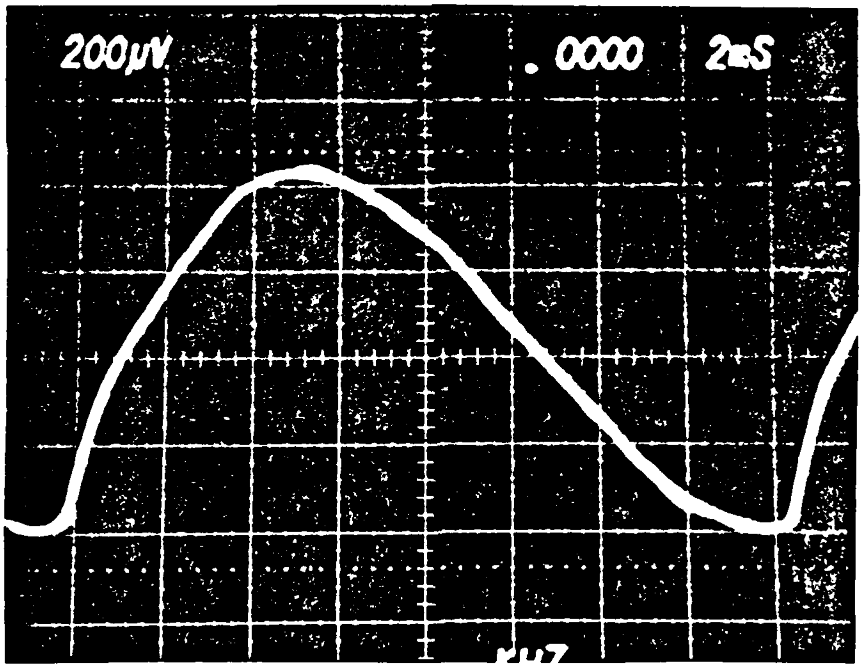

(b)

Figure 3.12. Time response of the transmittance of a pixel
a) for minimum brightness setting,
b) for maximum brightness setting.

Possible Improvements

It may be possible to modify the LCTV, for minimal cost, to perform better as a spatial light modulator. Since the blackest 'dark screen' was obtained at the minimum brightness setting, it seems reasonable that this is the best place to operate the LCTV. At this brightness setting, however, the bright pixel voltage was too small to give a really bright pixel. It may be possible to obtain a greater dynamic range if the voltage swing of the segment electrode pulse were to be increased so that the dark screen voltage would be as low as it is for the minimum brightness setting, while the bright screen voltage was higher as it is at the 75% setting. This would give a higher dynamic range, but there would be a trade-off; the bright pixels would not recover to their dark state before the next excitation interval. Because of this, the display of the LCTV would not be able to adapt to a rapidly changing input as well as it presently could. This modification, therefore, would only be useful when slowly varying images were to be displayed.

Conclusions

In this chapter, the construction, operation, modifications to, and performance of the LCTV have been discussed. It was found that with minor modifications, the low-cost LCTV could be made to perform quite well as a spatial light modulator for a laser. While the performance

may not be good enough for military system application, it does show that the technology involved in building such a television, could be used for such devices. The low-cost television itself can, easily, be of great value in the laboratory as well as an instructional tool for education in the principles of spatial light modulators.

The next chapter will discuss the experimental set-up used for the remainder of the thesis which involved the use of the LCTV in an optical processor. The LCTV was used as an input transparency for an optical edge enhancer as well as an optical filter in the Fourier transform plane of the optical processor.

IV. Experimental set-up

This chapter will describe the optical equipment and instruments used in the experimental portion of the thesis. The way in which the optics were set-up will be described for each experiment as well as some of the techniques used for taking measurements and data. In the first section the set-up for deriving the collimated beam which was used throughout the research will be discussed. The second section addresses the optical set-up used for the characterization of the LCTV. This is followed, in the third section, by a description of the optical set-up for the Fourier transforming and inverse Fourier transforming processor. This section also covers the edge enhancement by spatial filtering. The last section describes the set-up used for investigating the edge enhancement by image cancellation.

Laser/collimating set-up

Before any of the experiments involving the spatial light modulator (SLM) could be conducted, a collimated laser beam with a sufficiently large cross section was needed. The laser used throughout the experiments in this thesis was a Spectra-Physics model 125A helium-neon laser. The beam from this laser was focused onto a pinhole by a lens. The

pinhole was placed in the front focal-plane of a collimating lens to produce a 12-cm diameter collimated beam. This collimating set-up is shown in Figure 4.1. In order to keep the beam on the work table, the mirrors shown were used. Since the collimated beam was larger than the screen size of the SLM's, the aperture shown before the second mirror was used. The aperture passed the most uniform portion of the beam to be used with the SLM's, while blocking the unneeded light. This collimated light set-up was used throughout the experiments.

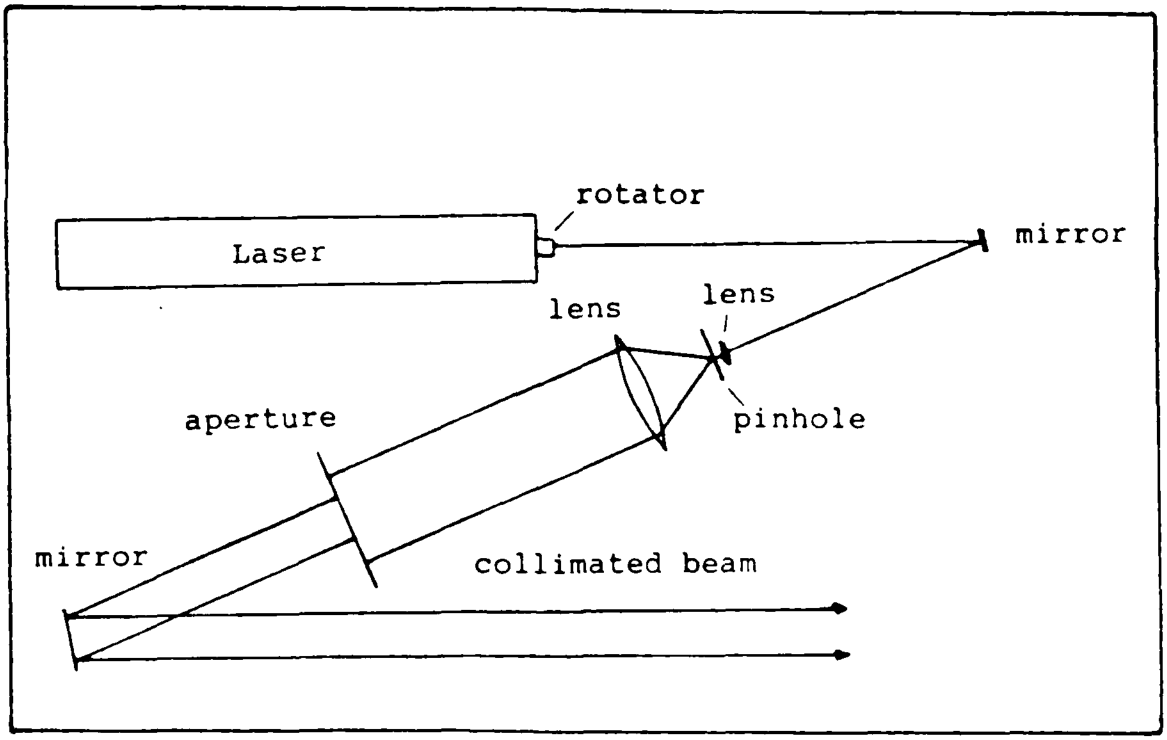

Figure 4.1. Experimental set-up for collimated light.

LCTV characterization

The liquid crystal television (LCTV) was placed into the collimated beam as shown in Figure 4.2. Two 10-cm diameter polarizers were placed in the beam also, one before and one after the LCTV. These polarizers could be rotated to any angle desired. The orientation of the plane of polarization of the collimated beam was set by a rotator mounted on the laser itself; it was adjusted so that the light impinging on the LCTV was polarized at an angle of 45° from vertical. This angle was found to give the best "dark" screen with the LCTV turned off.

Due to imperfections in the optical set-up, however, the polarization of the collimated beam was not perfect by the time it reached the LCTV. The slight imperfections were removed by placing the first polarizer in front of the LCTV. This polarizer also allowed small changes in the input polarization to be made without changing the orientation of the rotator on the laser. The second polarizer was used as the analyzer for the LCTV.

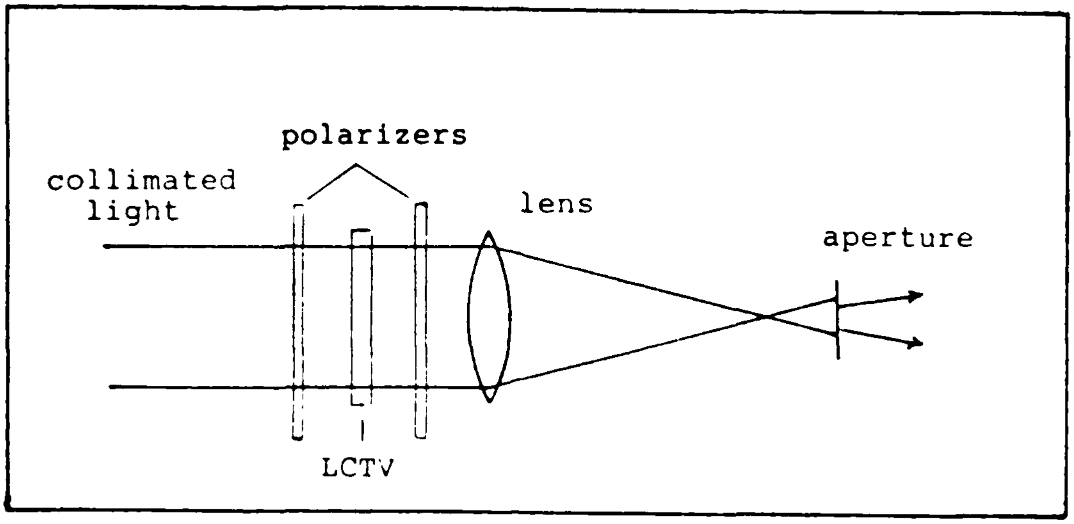

Figure 4.2. Experimental set-up showing position of LCTV.

The LCTV was driven by an Apple II+ personal computer for much of the experiments. The Apple computer was operated in the high resolution graphics mode and the video output from the computer was connected directly to the video input jack on the LCTV. This allowed for the display of a variety of binary images on the LCTV during the experiments.

A lens was placed after the LCTV as shown in Figure 4.2. This lens was used to focus the screen from the LCTV onto a light meter for comparing the intensity of the light passed by a "bright" screen with that passed by a "dark" screen. The aperture was used to mask off parts of the display which were not addressed by the computer.

The light meter was replaced with a vidicon camera for the dynamic range measurements. The vidicon camera was used as an input to a video analyzer. The video analyzer was an

Interpretation Systems Incorporated model VP-8 image analyzer. The lens and camera were positioned so that the individual pixels of the LCTV display were easily discernible on the video analyzer. The video analyzer then provided relative measurements of the intensity difference between a pixel in the on (transmissive) state and a pixel in the off state. The video analyzer measured the average brightness of the video at a point indicated by the position of cross-hairs on a television monitor. The indicated value had a bias value which was present even when no light was entering the camera. This bias value had to be subtracted from the intensity values for the brightness of the pixels to obtain the dynamic range.

The technique used to take the measurements was as follows: Part of the display which was imaged onto the camera was masked so that no light entered the camera. This portion was used to normalize the values of the intensities. The brightness control on the LCTV was set at the maximum position. A voltmeter connected between the wiper arm and the positive voltage end of the brightness control potentiometer was used to indicate the position of the control. The orientations of the input polarizer and the analyzer were then adjusted to give the lowest intensity readings for a pixel in the "off" state. This intensity value was recorded. The pixel was then turned on and the resulting intensity value was recorded. The bias value was subtracted from both "on" and "off" intensity values and a

ratio of the resulting numbers taken. To convert this contrast ratio to decibels the formula $10 \cdot \log(R)$ was used where R is the contrast ratio. This procedure was repeated for incremental positions of the brightness control.

In order to measure the time response of the pixels to the applied voltage the video analyzer was replaced with a photodiode. The lens and photodiode were positioned so that only one pixel was imaged onto the photodiode. The output of the photodiode was used as an input to an oscilloscope. As in the dynamic range experiments the response was measured as a function of the setting of the brightness control potentiometer. The polarizers were also positioned for the optimum contrast ratio (or darkest "off" pixel) for each setting of the brightness control.

Optical processor

Once the characterization of the LCTV was complete the next step was to use the LCTV in an optical processor. The first set-up used was the dual Fourier transforming processor shown in Figure 4.3. The LCTV was placed, along with its associated polarizers, in the collimated beam in front of a Fourier transforming lens. A microscope objective was placed behind the first lens to expand the scales of the Fourier transform so that the spatial filtering task was easier. The second Fourier transforming lens was identical to the first and it was also followed by a microscope objective to enlarge the resulting image. The

microscope objectives are shown in Figure 4.3 as small lenses after the larger transforming lenses. This resulting image was also observed by imaging it onto the vidicon camera mentioned earlier.

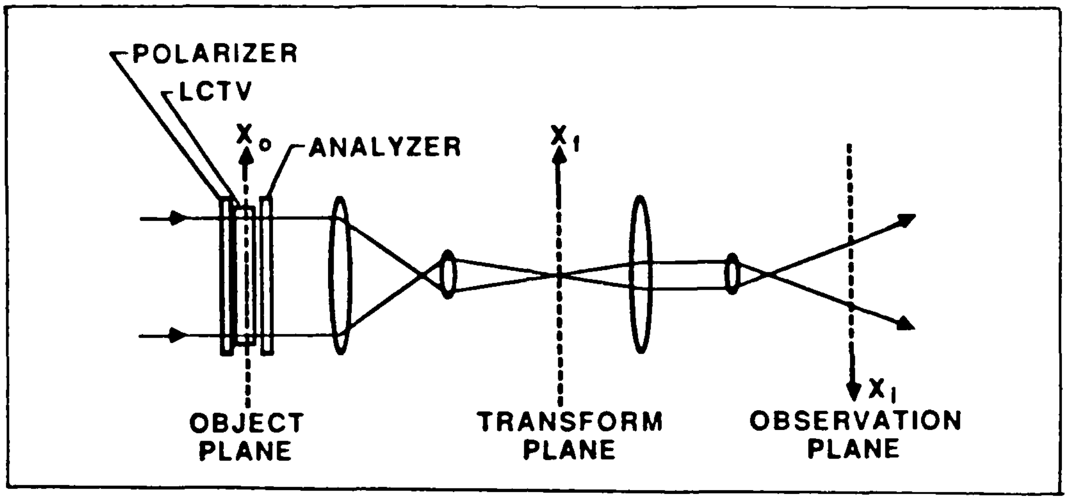

Figure 4.3. Experimental set-up showing dual Fourier transforming processor.

Image cancellation

The same Fourier transforming optical processor was used in the image cancellation experiments. For these experiments, though, a second LCTV was placed behind the second Fourier transforming lens set as shown in Figure 4.4. Instead of displaying the image on just one LCTV in the object plane, the second LCTV is used with the same video input. The polarizers of the second LCTV, though, are adjusted so that the resulting image is the negative (in the photographic sense) of the first. The extra two lenses shown before the second LCTV are used to invert the image, after passing through the second Fourier transforming lens,

so that it is right-side up as it impinges on the second LCTV.

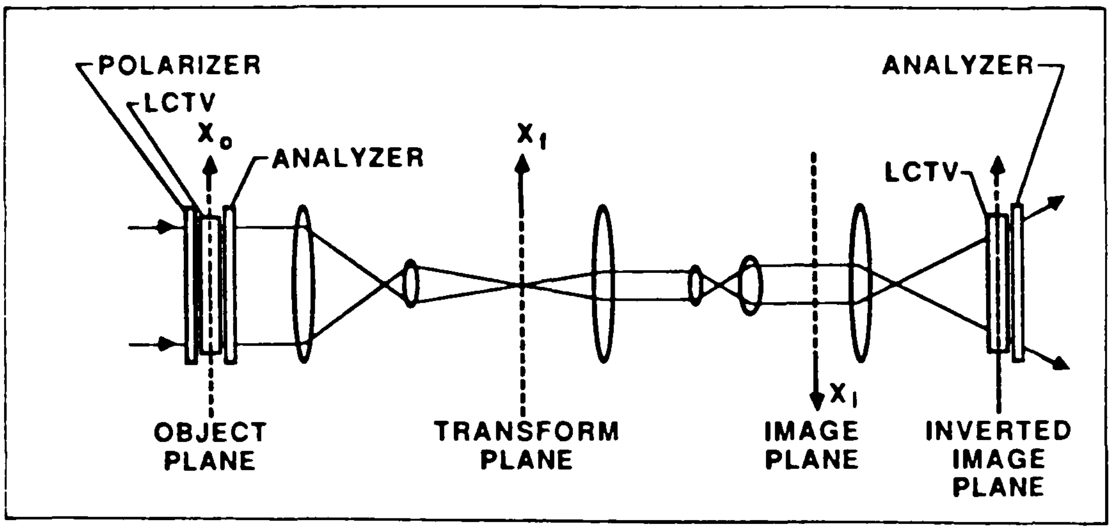

Figure 4.4. Experimental set-up for image cancellation.

Since only two of the large polarizers were available, the analyzer from the first LCTV was moved and used as the analyzer for the second LCTV. A smaller polarizer was placed after the first microscope objective and used as the analyzer for the first LCTV. This polarizer was adjusted so that the image from the first LCTV was the inverse of the image generated by the Apple computer. This was done simply by orienting the polarizer to block the light passed by the on pixels and pass the light rotated by the off pixels. The analyzer behind the second LCTV was oriented so that the image impressed on the laser light by the second LCTV was the same as that generated by the computer. When the inverted image from the first LCTV impinged on the second LCTV the two transmittances multiplied as discussed in

chapter two. The result was a small intensity value from one display multiplied by a large intensity value from the other. As long as the two images were in registration, and the polarizers were adjusted properly the two images would cancel each other.

In order to blur the first image as it impinged on the second LCTV, spatial filtering was used in the Fourier transform plane again, as was done for the high-pass filtering method. In this case, though, the higher spatial frequencies were filtered rather than the lower ones. This blurred the edges from the first image and the result was the edges of the image.

Conclusions

As mentioned earlier, this chapter only deals with the experimental set-up used in the research and does not discuss the results of these experiments. The collimating set-up was described, followed by the set-up used to characterize the LCTV via an image analyzer and other test equipment. Some experimental techniques were discussed along with the LCTV characterization set-up. The generic optical processor which was the central part of much of the experimental work was described along with the set-up used in the image cancellation experiments. The next chapter will discuss the results which were obtained by using these optical set-ups for edge enhancing images which were displayed on one of the LCTVs.

V. Experimental results

This chapter details the results of the experiments described throughout this thesis. Since most of the experiments dealt with edge enhancement, the results will be shown photographically. The first section of this chapter, though, deals with the characterization of the LCTV. Whereas chapter three covered the operation principles of the LCTV in agonizing detail, this section will only discuss the performance of the LCTV as measured in the experiments. Some of these measurements were discussed in chapter three and will not be repeated here. The following two sections will deal with the results of the spatial filtering method of edge enhancement with one section dealing with using the LCTV as the input image and the other with using the LCTV as the spatial filter. The fourth section discusses the image cancellation method results. An additional section was added to discuss a third method of edge enhancement which was found during the course of the experimentation.

LCTV specifications

One of the first experiments on the LCTV was to measure the amount of rotation the display caused to the incident light. This was measured with the power to the LCTV off. The rotation was measured by finding the best dark screen by

adjusting both polarizers and comparing the angles of the two polarizers. It was found that the display did not rotate the light exactly 90° as predicted, but rather only about 55°. The variation from 90° is probably due to non-uniformities in the alignment of the liquid crystal molecules at the two glass plates.

Another experiment was run to determine the amount of effective rotation between the bright screen and a black screen. This was accomplished by imaging the screen onto a light meter and first finding the best dark screen by adjusting the polarizers. The screen was then driven bright and the second polarizer was adjusted to find the best null for the bright screen. The difference between the two settings of the second polarizer is the effective rotation. This difference was found to be 23° at the optimum setting of the brightness control (75%) and it varied down to 2° at the minimum brightness setting.

A second LCTV was also needed for the image cancellation experiments which will be discussed later. This second LCTV, though, was not inserted into a liquid gate like the first one was. For the second LCTV, the liquid gate was replaced by gluing optical flats onto the front and back of the display (14:1381). The optical flats used were actually holographic plates which had been cleaned and cut to the appropriate size. The glue used was Norland Optical Adhesive number 61. This adhesive is ultravioletly cured and formed a solid, clear bond. The glue did as well

as, if not better than, the liquid gate at matching the index of refraction of the glass to remove the optical imperfections. The performance of the two methods of removing the imperfections were compared only by comparing the Fourier transforms of the two LCTVs. There was no observable difference between the transform of the LCTV with the plates glued on and that of the LCTV in the liquid gate. The LCTV with the optical flats glued on was much easier to handle and work with than the one in the liquid gate which makes the glue method preferable.

In the last chapter, it was mentioned that the LCTV was driven by an Apple II+ computer. There was one problem with using this computer to generate the video for the LCTV. This was in the number of pixels addressed by the computer and the number of pixels in the LCTV display. The Apple computer generates 192 vertical pixels and 280 horizontal pixels. These pixels are displayed on the LCTV on 96 vertical pixels by 111 horizontal pixels. This produces no problem in the vertical direction, since there is an exact 2:1 ratio. The LCTV just displays every other line of video generated by the computer. In the horizontal direction, though, there is not an even ratio. This causes an edge blurring of vertical edges on the LCTV (4: 245). The circuitry in the LCTV cannot consistently address the same pixels in the horizontal direction at the edges of an image. This results in what appears as the edges "crawling" in the vertical direction. Other computers were tried, but the

same problem existed. It was not judged to be of any serious consequence to the thesis so it was tolerated.

Edge enhancements with LCTV as input object

The dual Fourier transforming set-up described in the last chapter was used to experiment with edge enhancing by spatial filtering. In these experiments, the LCTV was used to generate the input image and a small opaque spot was placed onto a plate of glass in the Fourier transform plane. This small spot was the high-pass filter. The size of the spot was of the same order as the size of the airy disc generated in the transform plane with no input image or LCTV in the object plane. The results of this edge enhancement are shown in Figure 5.1. In this figure, the edge enhancement is shown with the high-pass filter combined with an aperture. The aperture was used to eliminate the high frequencies associated with the grid structure of the LCTV drive lines, it was positioned so that only the central lobe of the transform was passed.

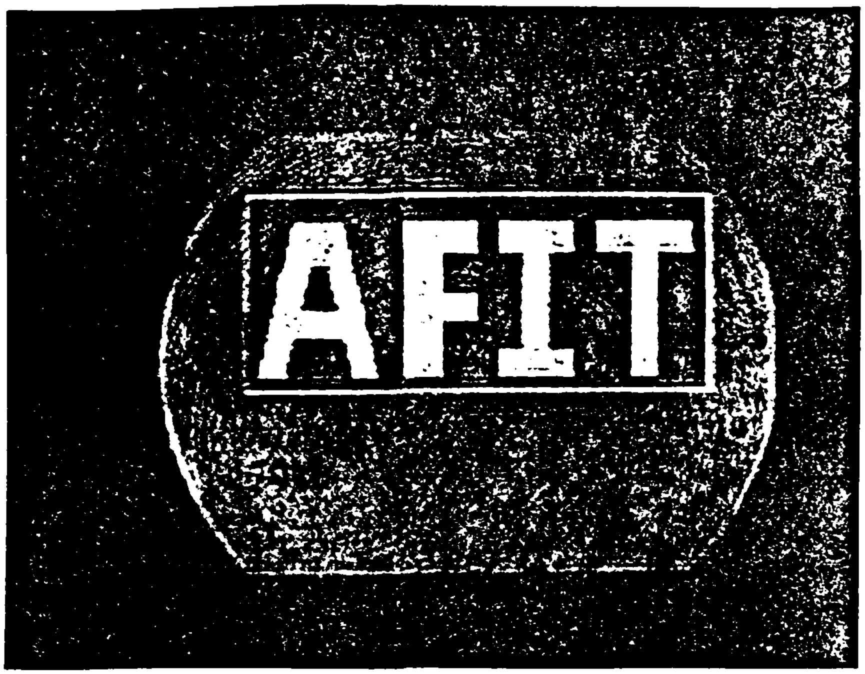

(a)

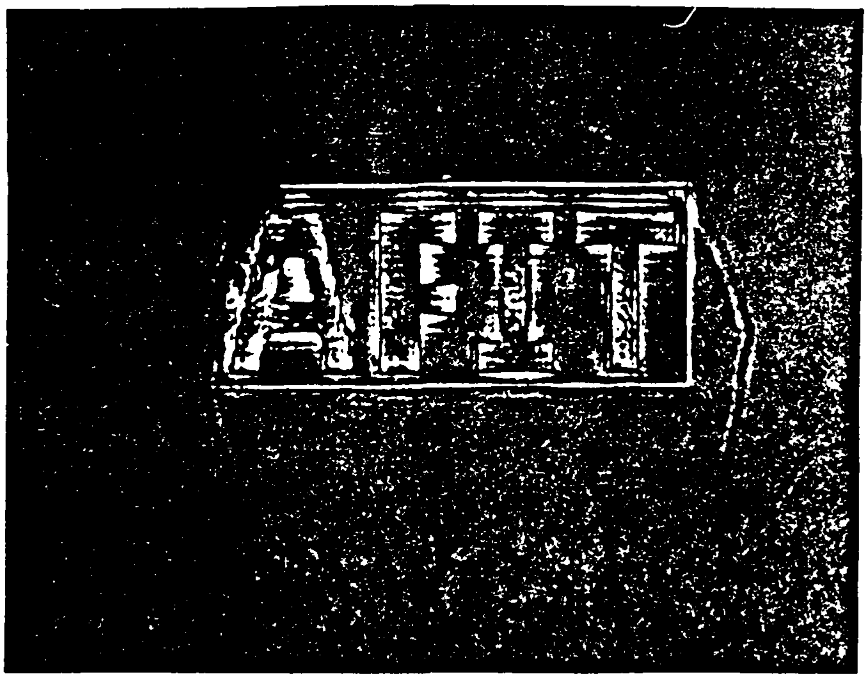

(b)

Figure 5.1. Edge enhancement by high-pass spatial filtering, a) original image, b) edges of image.

Edge enhancements with LCTV as filter

The high-pass spatial filtering method was done again, but this time with the LCTV as the filter instead of the input object. The same metal cut-out that was used in the photographs in chapter two was used here for the input image. The LCTV was placed into the Fourier transform plane as the filter. Recall from chapter two that the resulting image in the observation plane is the convolution of the input image with the Fourier transform of the filter. This causes a repetition of the input image due to the periodic nature of the Fourier transform of the LCTV (see Figure 3.7). This repetition of the resulting image can be seen in Figure 5.2. This figure shows the resulting image with the LCTV turned off so there is no high-pass filtering. Figure 5.3 shows an expanded view of the small dot which was used as the spatial filter on the LCTV. Figure 5.4 shows the results of this spatial filtering. Most of the effects of the periodic nature were masked out by placing an aperture before in the observation plane just large enough to pass the original image.

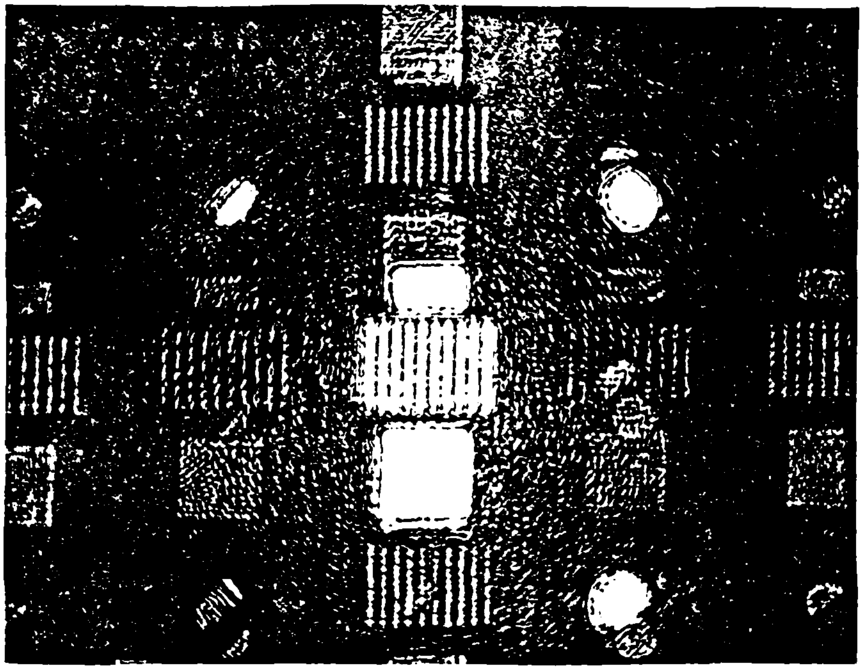

Figure 5.2. Convolution of the input image with the Fourier transform of the LCTV.

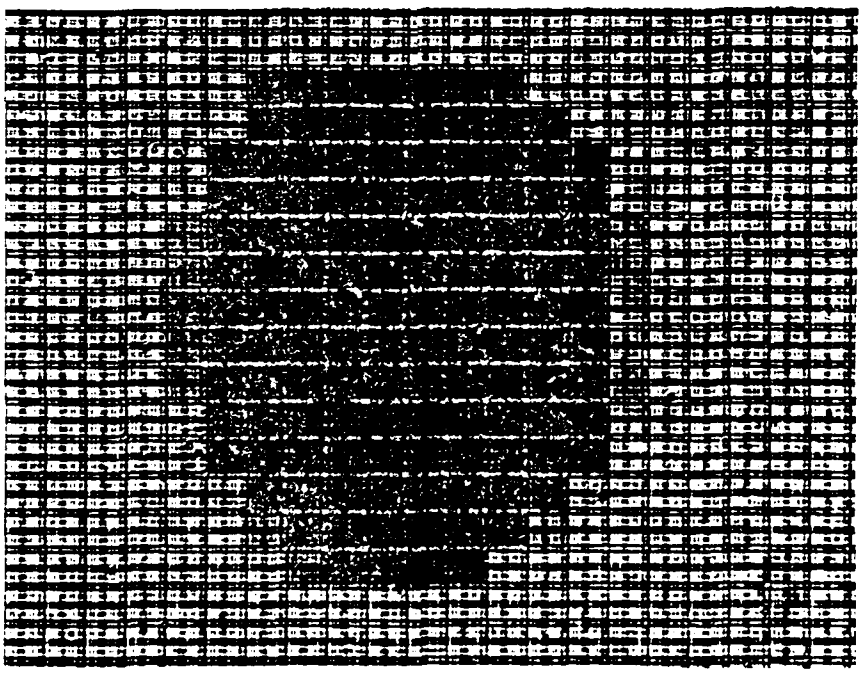

Figure 5.3. Spatial filter used on the LCTV.

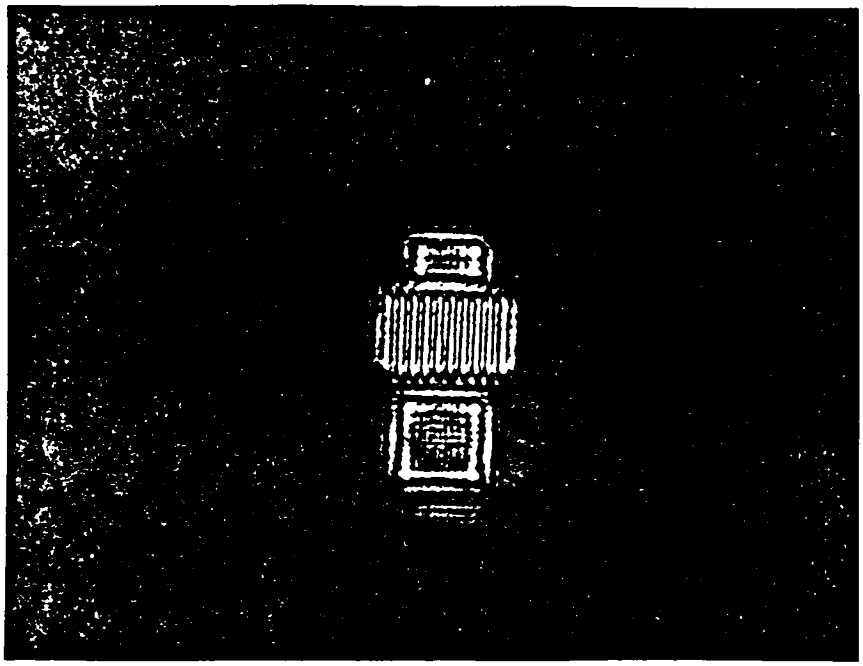

Figure 5.4. Edge enhancement by high-pass spatial filtering with LCTV as the filter.

Image cancellation

The second method of edge enhancement, the image cancellation method was described in the last chapter and the set-up was shown in Figure 4.4. The results can be seen in Figure 5.5. In this figure, the original image was larger than the 'AFIT' used in Figure 5.1, but shows a slightly blurry edge on all the edges. Figure 5.6 shows this method on the same 'AFIT' image used earlier. This image shows that the edges obtained with the image cancellation are not uniform and are wider than those seen with the spatial filtering. In the second image, some of the edges run together on the narrower portions.

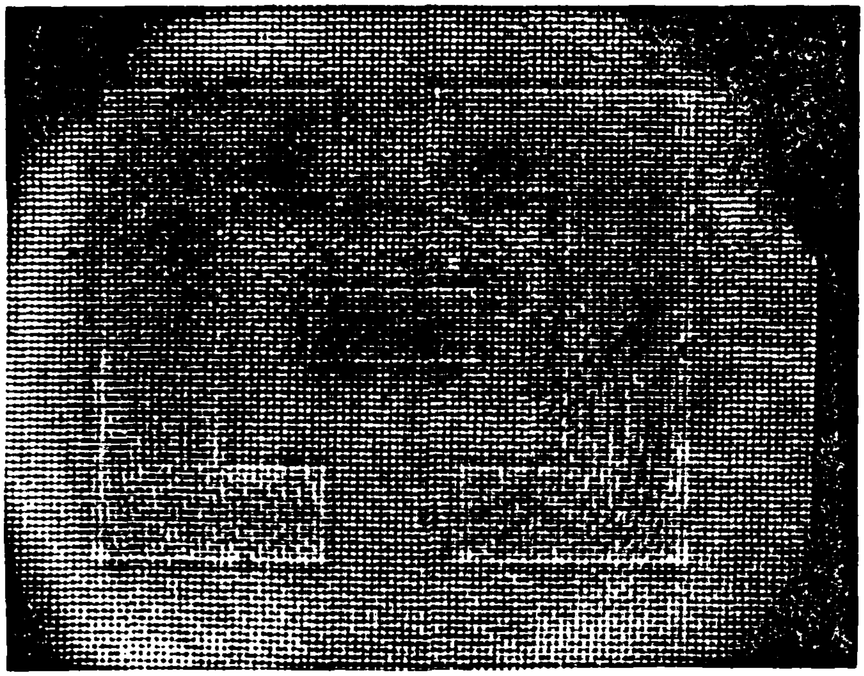

Figure 5.5. Edge enhancement by image cancellation.

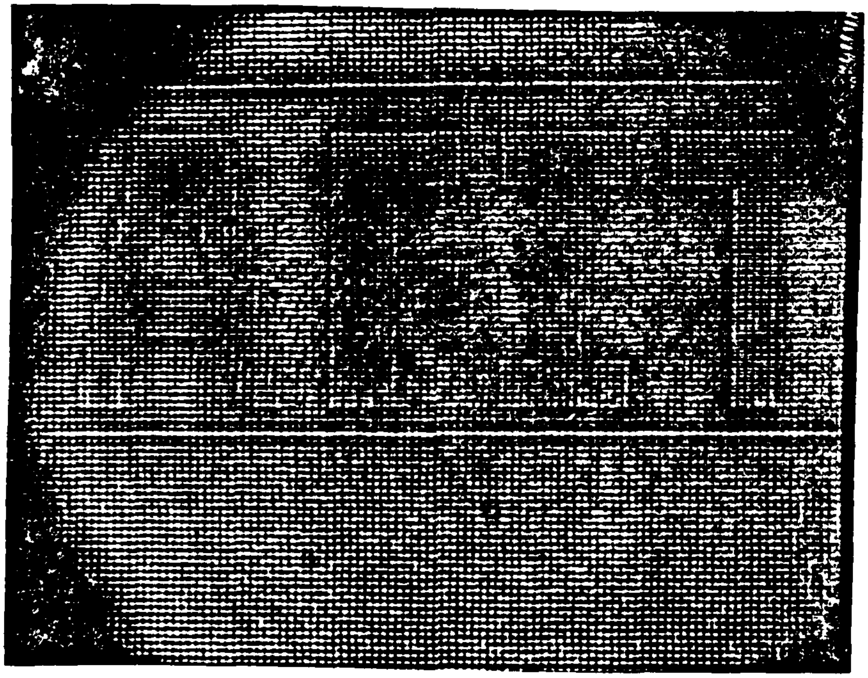

Figure 5.6. Edge enhancement of an image with narrow segments.

Phase-only edge enhancement

The third and final method of edge enhancement is one which was found during the course of the experiments. It was, therefore, not discussed under the background in chapter two. This method uses the same set-up as the spatial filtering method with the LCTV as the input. In this method, the polarizers for the LCTV are adjusted so that the LCTV is phase modulating the light rather than amplitude modulating. This is accomplished by orienting the second polarizer (analyzer) so that it is at the midpoint of the effective rotation between the polarization of the 'on' pixels and the polarization of the 'off' pixels. With this setting of the analyzer, the light from the 'on' pixels will differ from the light from the 'off' pixels only by a phase component of π radians (4:246). Although the set-up from Figure 4.3 was used, no spatial filtering was done. The reason for this set-up was that by adjusting the position of the second microscope objective, the resulting image could be blurred. When the image is blurred in this manner, the areas with opposite phase components overlap at the edges of an object and interfere with each other. This leaves the image with only the edges visible. The edges from this method are black edges as compared to the bright edges from the first two methods. These black edges can be seen in Figure 5.7

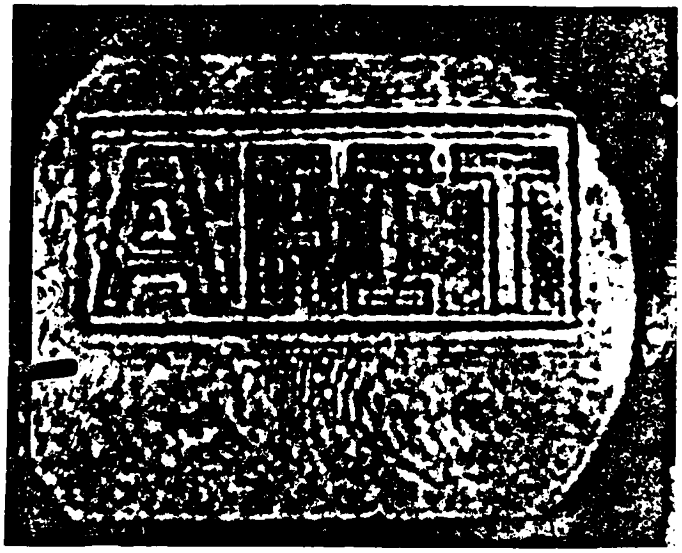

Figure 5.7. Edge enhancement by phase cancellation.

Incoherently illuminated objects

Another experiment performed was to use a video camera instead of the computer as the input to the LCTVs. This was done to compare the three methods when various gray levels are present rather than the binary data generated by the computer. For this experiment, a photo of an SR-71 aircraft was imaged via a television camera onto the LCTVs. The results are shown in Figures 5.8 through 5.10.

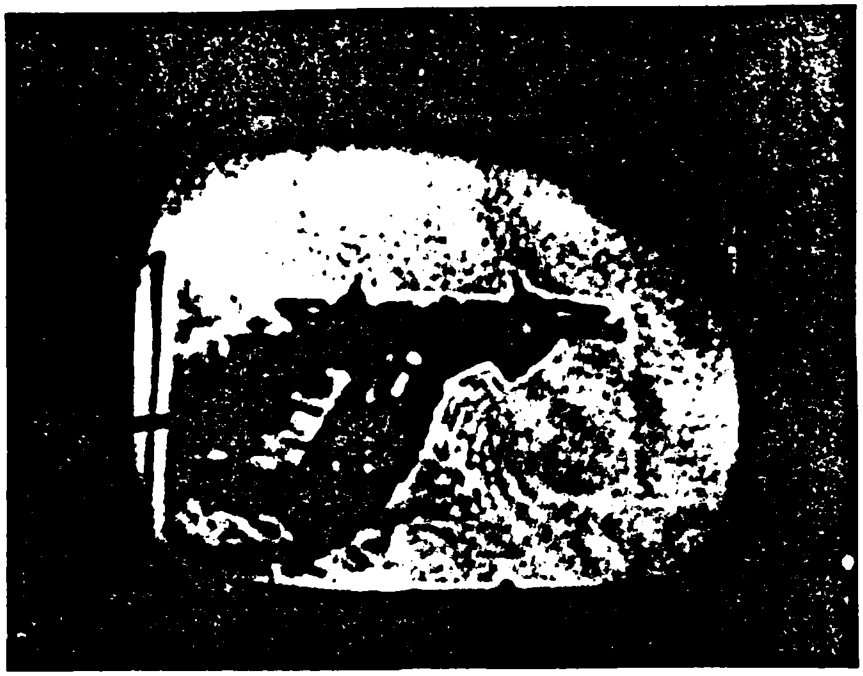

(a)

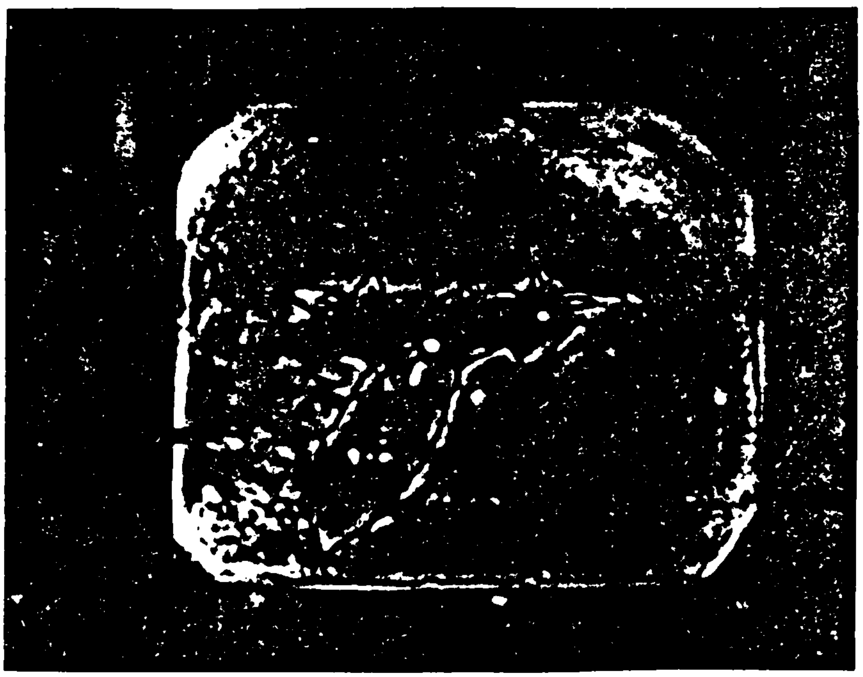

(b)

Figure 5.8. Edge enhancement by high-pass spatial filtering, a) original image, b) filtered image.

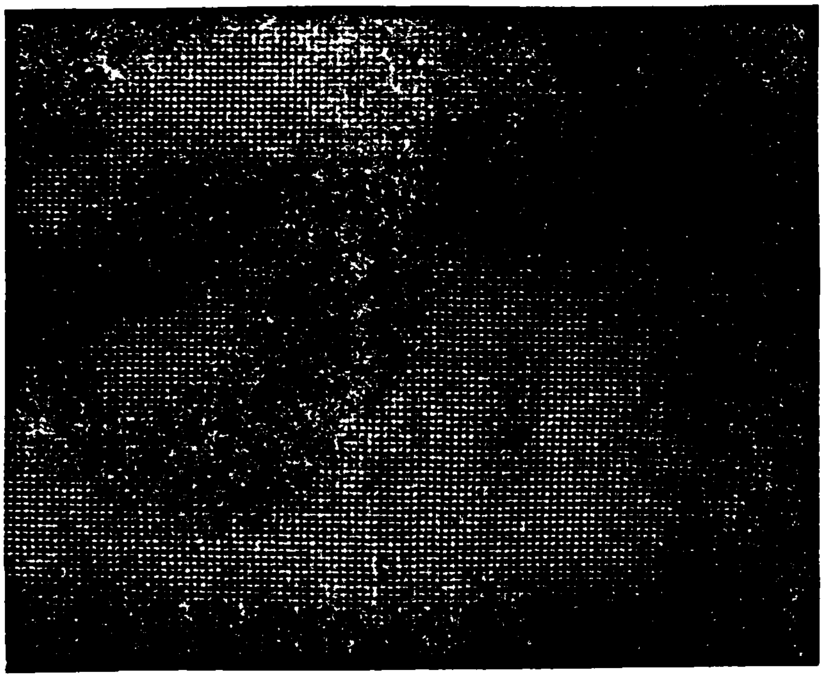

Figure 5.9. Edge enhancement by image cancellation.

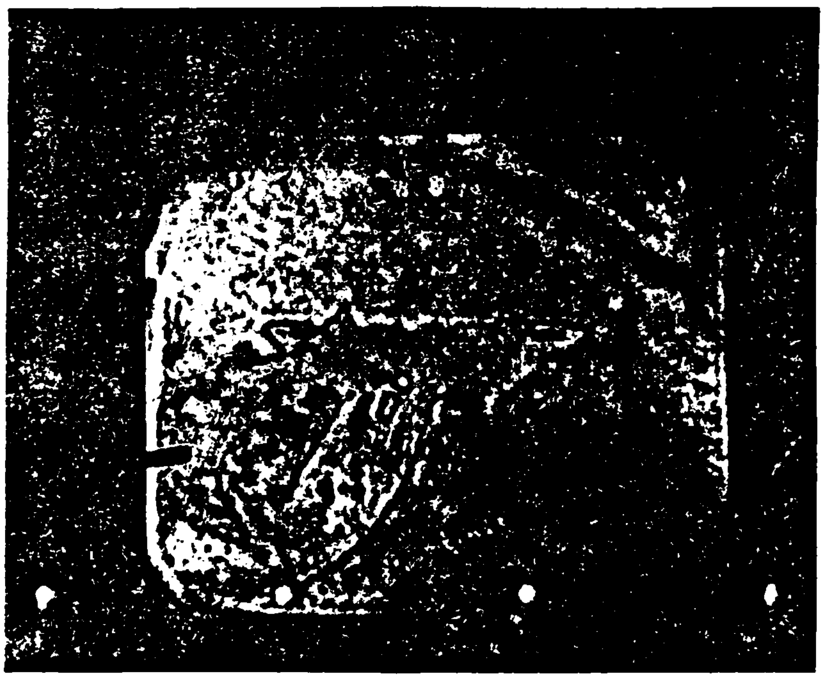

Figure 5.10. Edge enhancement by phase cancellation.

Conclusions

In comparing the three methods of edge enhancement, some characteristics of each method need to be pointed out.

The edge enhancement by spatial filtering leaves a bright line on each side of the actual edge, which appears as a dark line. This is due to a phase reversal which takes place at the edge resulting from the convolution of the image with the transform of the spatial filter. This double line is not present in either the image cancellation or phase methods. The image cancellation method leaves a single bright edge, but the edge is blurred on the inside of the object and is not uniform. The phase method leaves a single uniform black edge.

This chapter has presented the end results of the research which was discussed in chapters two through four. The specifications of the LCTV investigated were presented along with two different methods of using the LCTV in an optical edge enhancer. First the results of using the LCTV as the input object in the enhancer were presented followed by the results of using the LCTV as the spatial filter in the same type of edge enhancer. The results of the image cancellation method were also presented. Another method of edge enhancement was presented which was discovered during the course of the research; the phase only method. This method was not discussed in the background chapters since it was not the object of the research, but it was found to give very interesting results. The edges obtained from this method were relatively sharp, and easily discernable. Finally, the results of edge enhancing an image derived from an incoherent image via a television camera were presented.

This was done for all three methods. The next and final chapter will wrap up all of these experiments with some conclusions and recommendations for follow-on research.

VI. Conclusions

The suitability of a low-cost liquid crystal television (LCTV) to function as a spatial light modulator has been investigated, along with an application of using such a modulator in an optical pre-processor. The particular pre-processor application investigated was that of optically enhancing the edges of an image before it is used as an input to an electronic pattern recognition system.

Summary

The advantages of using optical processors in such an application, mainly the speed at which an optical processor can operate have been discussed. Recall that an image can be processed optically in nano-seconds whereas an electronic processor may take milliseconds or even seconds. The theory of how the optical processor functions and how the edge enhancements are be accomplished has been discussed along with a detailed account of the construction and operation principles of the LCTV used. There was a discussion of the modifications made to the LCTV and its performance as a spatial light modulator was measured.

The LCTV was modified to make it open 90° along with removing the diffuser, protective plastic plate and original polarizers. Two methods of correcting for the imperfections

in the optical flatness of the display were used, the liquid gate and gluing optical flats to the display. These, however, are not the only methods available for correcting for these imperfections. One other method which may warrant further investigation, is to use holographic correction on the display (2:398). This method could possibly give better performance than either of the methods used here since both the liquid gate and the gluing method, can only compensate for the imperfections on the outside of the display and cannot compensate for imperfection on the inside of the display.

To summarize the results of the edge enhancement experiments, it would appear that any of the three methods of edge enhancement will produce recognizable edges of a given image. The spatial filtering method and phase cancellation methods appear to present the more usable edges since the image cancellation method produces edges which are more blurry and less uniform than the other two methods. Both of these methods produce easily discernible edges, but the spatial filtering method produces a double edge rather than a single edge. The phase method leaves a single uniform black edge, but it is slightly blurred when compared to the original image.

All of these methods performed the edge enhancement task whether the image was binary, as in the computer generated image, or was continuous as from a television camera. The capability of enhancing images generated by a

television camera allow continuous, real-time enhancing of any scene, even if the objects in the image are in motion. This capability could make these methods of edge enhancement of value in an optical pre-processor for an automated pattern recognition system.

The spatial light modulator constructed of the LCTV did have its draw-backs. The most prominent of these is the low dynamic range or contrast ratio. The LCTV had only about 10 dB of dynamic range as compared to higher cost spatial light modulators which can offer as much as 30 dB. The other most troublesome characteristic of the LCTV was its sensitivity to the polarization angle of the incident light. This was most prominent in the set-up for image cancellation. Since the analyzer for the first LCTV must be oriented for the best picture on LCTV-1, the resultant polarization of the light may not be best for LCTV-2, reducing its dynamic range as mentioned in chapter three. The last significant problem was the number of pixels in the display. The number of pixels in the display did not provide as much resolution as may be required by some tasks, but it was sufficient for the experiments performed in the laboratory. These factors may prevent these low-cost LCTVs from being suitable for use in a commercial pattern recognition system, but the techniques of edge enhancement discussed in this paper will work with any spatial light modulator which operates on polarization rotation.

Other Applications

The application of the optical pre-processor described in this thesis is by no means the only one for which the optical processor could be used in the pattern recognition problem. Optical processing offers the possibility of performing other tasks optically such as the correlation of images with known objects (6:177). A correlator can be used in an automatic target recognition system by itself, completely eliminating the need for electronic image processing. Spatial light modulators can perform in such a correlator, as both the input image (as in the application discussed in this thesis) as well as the filter containing the transform of the known object which is being correlated (5:466). It is unknown whether or not the the LCTV used in this thesis may is capable of performing these tasks, but this application is one which should be further investigated as a follow-on to this thesis.

It should also be mentioned that the performance of pattern recognition software using the edges of images obtained through optical methods has not been compared with the performance using edges obtained through electrical image processing. There is, therefore, no information to indicate whether the pattern recognition software will perform better or worse with an optical edge enhancer than with an electrical one, and more work is needed in this area. Optical processing, though, offers a promising alternative to all digital processing in pattern

recognition. The future may well show optical target detectors and robot vision systems composed of a hybrid of optical processors and digital processors.

BIBLIOGRAPHY

1. Blinov, Lev Mikhaylovich. Electro-optical and magneto-optical properties of liquid crystals. Translation of: Elektro- i magnitooptika zhidkikh kristallov. John Wiley & Sons Ltd. 1983.

2. Casasent, "Phase Correction of Light Modulators," Optics Letters, 11: 398-400 (June 1986).

3. Cornsweet, Tom N. Visual Perception. New York: Academic Press, 1970.

4. Davis, Jeffrey A. and others. "Applicability of The Liquid Crystal Television For Optical Data Processing," Proc. SPIE, 613-41: 245-254 (1986)

5. Flannery, David L. and others. "Real-time coherent correlator using binary magnetooptic spatial light modulators at input and Fourier planes," Applied Optics, 25 (4): 466 (February 1986).

6. Goodman, Joseph W. Introduction to Fourier Optics. San Francisco: McGraw-Hill Book Company, 1968.

7. Lee, Sing H. "Optical implementations of digital algorithms for pattern recognition," Optical Engineering, 25 (1): 069-075 (January 1986).

8. Lee, Sing H. and others. "Two-dimensional Silicon/PLZT Spatial Light Modulators: design Considerations and Technology," Optical Engineering, 25 (2): 250-260 (February 1986).

9. McIlroy, C. D. and others. "Edge Detection in Real-Time," SPIE, 504: 445-454 (1984).

10. Parrish, E. A. Jr and others. "Integrated Optical Processors In Pattern Recognition," Pattern Recognition, 18 (3/4): 227-23[illegible] (February [illegible]).

11. "Realistic Service Manual," for [illegible] 2.7 inch pocketable Black and White [illegible] Television model [illegible].

12. Schowengerdt, Robert A. [illegible] Processing and [illegible]. Orlando: Academic Press, [illegible].

13. Sherman, Rand C. and others. "Hybrid incoherent optical pattern recognition system," Applied Optics, 22 (22): 3579-3582 (November 1983).

14. Tai, Anthony M. "Low-cost LCD spatial light modulator with high optical quality," Applied Optics, 25 (9): 1380-1382 (May 1986).

15. Upatnieks, Juris. "Portable real-time coherent optical correlator," Applied Optics, 22 (18): 2798-2803 (September 1983).

16. Young, Matt. "Low-cost LCD video display for optical processing," Applied Optics, 25 (7): 1024-1026 (April 1986).

Vita

Kenneth D. Hughes was born at Cheboygan Michigan, on 4 August 1959. He graduated from Burt Township High School in Grand Marais Michigan in 1977. Having earned an Air Force R.O.T.C. scholarship, he attended Michigan Technological University in Houghton, Michigan, graduating in May 1981, with honor. He received the degree of Bachelor of Science in Electrical Engineering, specializing in communications and electronics. His Air Force specialty code is 4934 (a communications/electronics officer) having attended the Communications-Electronics officers course at Keesler AFB, Biloxi Mississippi. Following his assignment to Keesler AFB, he was assigned to the Foreign Technology Division at Wright-Patterson AFB, OH. He served at the Foreign Technology Division for two and one half years before entering the School of Engineering, Air Force Institute of Technology, in June of 1985. He enrolled in the curriculum of Communications/Radar/Optical Information Processing.

Permanent address: P.O. Box 316

Grand Marais, MI 49839

UNCLASSIFIED

SECURITY CLASSIFICATION OF THIS PAGE

REPORT DOCUMENTATION PAGE

1a. REPORT SECURITY CLASSIFICATION	UNCLASSIFIED
1b. RESTRICTIVE MARKINGS	
2a. SECURITY CLASSIFICATION AUTHORITY	
2b. DECLASSIFICATION/DOWNGRADING SCHEDULE	
3. DISTRIBUTION/AVAILABILITY OF REPORT	Approved for public release distribution unlimited
4. PERFORMING ORGANIZATION REPORT NUMBER(S)	AFIT/GE/ENG/86-D-6
5. MONITORING ORGANIZATION REPORT NUMBER(S)	
6a. NAME OF PERFORMING ORGANIZATION	School of Engineering
6b. OFFICE SYMBOL (If applicable)	AFIT/ENG
7a. NAME OF MONITORING ORGANIZATION	
6c. ADDRESS (City, State and ZIP Code)	Air Force Institute of Technology Wright-Patterson AFB, OH 45433
7b. ADDRESS (City, State and ZIP Code)	
8a. NAME OF FUNDING/SPONSORING ORGANIZATION	Avionics Laboratory
8b. OFFICE SYMBOL (If applicable)	AFWAL/AADO
9. PROCUREMENT INSTRUMENT IDENTIFICATION NUMBER	
8c. ADDRESS (City, State and ZIP Code)	AFWAL/AADO Wright-Patterson AFB, OH 45433
10. SOURCE OF FUNDING NOS.	PROGRAM ELEMENT NO. / PROJECT NO. / TASK NO. / WORK UNIT NO.
11. TITLE (Include Security Classification)	See Box 19
12. PERSONAL AUTHOR(S)	Kenneth D. Hughes, Capt, USAF
13a. TYPE OF REPORT	MS Thesis
13b. TIME COVERED	FROM ____ TO ____
14. DATE OF REPORT (Yr., Mo., Day)	1986 December
15. PAGE COUNT	87
16. SUPPLEMENTARY NOTATION	

17. COSATI CODES		
FIELD	GROUP	SUB. GR.
17	08	

18. SUBJECT TERMS (Continue on reverse if necessary and identify by block number)

Pattern Recognition, Optical Images

Optical Processing, Image Processing

19. ABSTRACT (Continue on reverse if necessary and identify by block number)

Title: SUITABILITY AND APPLICATIONS OF LIQUID CRYSTAL TELEVISIONS IN OPTICAL PRE-PROCESSORS

Thesis Chairman: Steven K. Rogers, Captain, USAF

Approved for public release: IAW AFR 190-17.

LYNN E. WOLAVER

Dean for Research and Professional Development

Air Force Institute of Technology (AFC)

Wright-Patterson AFB OH 45433

20. DISTRIBUTION/AVAILABILITY OF ABSTRACT	UNCLASSIFIED/UNLIMITED ☒ SAME AS RPT ☐ DTIC USERS ☐
21. ABSTRACT SECURITY CLASSIFICATION	UNCLASSIFIED
22a. NAME OF RESPONSIBLE INDIVIDUAL	Steven K. Rogers, Captain, USAF
22b. TELEPHONE NUMBER (Include Area Code)	513-255-6027
22c. OFFICE SYMBOL	AFIT/ENG

DD FORM 1473, 83 APR EDITION OF 1 JAN 73 IS OBSOLETE

UNCLASSIFIED

SECURITY CLASSIFICATION OF THIS PAGE

The suitability of a low-cost liquid crystal television to function as a spatial light modulator for lasers is investigated along with an application of using such a modulator in an optical pre-processor for an electronic pattern recognition system. The particular pre-processor application investigated is that of optically enhancing the edges of an image. It was determined that the liquid crystal television could perform reasonably well as a spatial light modulator for applications where very high image quality was not required. Three different methods were found to produce recognizable edges of a given image: spatial filtering in the Fourier plane, image cancellation, and phase cancellation. The phase cancellation method was discovered during the course of the research. These methods were able to perform the edge enhancement task whether the image was binary as in a computer generated image, or was continuous as from a television camera.

END

4 - [illegible] - 87

DTIC